

A COMPARISON ATLAS OF ELECTRON AND
SCANNING ELECTRON FRACTOGRAPHY

A THESIS

Presented to
The Faculty of the Graduate Division

by

James Lee Hubbard

In Partial Fulfillment
of the Requirements for the Degree
Master of Science in Metallurgy

Georgia Institute of Technology

June, 1971

In presenting the dissertation as a partial fulfillment of the requirements for an advanced degree from the Georgia Institute of Technology, I agree that the Library of the Institute shall make it available for inspection and circulation in accordance with its regulations governing materials of this type. I agree that permission to copy from, or to publish from, this dissertation may be granted by the professor under whose direction it was written, or, in his absence, by the Dean of the Graduate Division when such copying or publication is solely for scholarly purposes and does not involve potential financial gain. It is understood that any copying from, or publication of, this dissertation which involves potential financial gain will not be allowed without written permission.

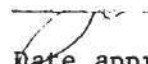
A handwritten signature, possibly "James", is written across a horizontal line that is part of a rectangular box.

7/25/68

A COMPARISON ATLAS OF ELECTRON AND
SCANNING ELECTRON FRACTOGRAPHY

Approved: _____

~~Chairman~~ _____

 Date approved by Chairman: 6-2-71

DEDICATED

To my loving wife, Eleanor, for her moral
support in completing this thesis

ACKNOWLEDGMENTS

The author wishes to express his sincerest gratitude to the following persons or organizations.

Dr. Niels N. Engel, thesis advisor, for his enthusiasm, guidance and patience during the course of this research.

Mr. John L. Brown, Senior Research Physicist in the Engineering Experiment Station, for the invaluable knowledge of microscopy he has given me during our eleven year association.

Dr. Robert F. Hochman for his interest and advice as a member of the thesis reading committee.

The Engineering Experiment Station for its partial support of this research.

Mrs. Ann Ortstadt for her aid in typing this thesis.

Due to the special requirements of this thesis, permission was granted by the Graduate Division to place figure captions for Figures 7-39 on the page preceding each figure.

TABLE OF CONTENTS

	Page
ACKNOWLEDGMENTS	iii
LIST OF ILLUSTRATIONS	v
CHAPTER	
I. INTRODUCTION	1
II. INSTRUMENTATION AND EQUIPMENT	6
Transmission Electron Microscope	
Scanning Electron Microscope	
III. PROCEDURE	13
Sample Marking	
Replication	
Transmission Electron Microscopy	
Scanning Electron Microscopy	
Stereoscopy	
IV. COMPARISON ATLAS	18
V. RESULTS AND CONCLUSIONS	97
LITERATURE CITED	100
OTHER REFERENCES	101

LIST OF ILLUSTRATIONS

Figure	Page
1. Schematic Drawing of a Transmission Electron Microscope	7
2. Schematic Drawing of a Scanning Electron Microscope	9
3. Diagram of a Secondary Electron Collector from a Scanning Electron Microscope	9
4. Stereo Adapter Parts for the SEM Stage	12
5. Stereo Adapter in Its Proper Position on the SEM Stage	12
6. Relative Positions of Two Points Before and After Tilting Through + and - the Angle θ	17
7. Comparison of TEM and SEM Fractography in Overload of Al Alloy	20
8. Comparison of TEM and SEM Fractography in Overload of Al Alloy	22
9. Comparison of TEM and SEM Fractography in Overload of Al Alloy	24
10. Comparison of TEM and SEM Fractography in Overload of Al Alloy	26
11. Comparison of TEM and SEM Fractography in Overload of Al Alloy	28
12. Comparison of TEM and SEM Fractography in Overload of Al Alloy	30
13. Comparison of TEM and SEM Fractography in Fatigue of Al Alloy	32
14. Comparison of TEM and SEM Fractography in Fatigue of Al Alloy	34
15. Comparison of TEM and SEM Fractography in Fatigue of Al Alloy	36

LIST OF ILLUSTRATIONS (Continued)

Figure	Page
16. Comparison of TEM and SEM Fractography in Fatigue of Al Alloy	38
17. Comparison of TEM and SEM Fractography in Stress Corrosion of Al Alloy	40
18. Comparison of TEM and SEM Fractography in Stress Corrosion of Al Alloy	42
19. Comparison of TEM and SEM Fractography in Stress Corrosion of Al Alloy	44
20. Comparison of TEM and SEM Fractography in Stress Corrosion of Al Alloy	46
21. Comparison of TEM and SEM Fractography in Overload of 4340 Steel	48
22. Comparison of TEM and SEM Fractography in Overload of 4340 Steel	50
23. Comparison of TEM and SEM Fractography in Overload of 4340 Steel	52
24. Comparison of TEM and SEM Fractography in Fatigue of 4340 Steel	54
25. Comparison of TEM and SEM Fractography in Fatigue of 4340 Steel	56
26. Comparison of TEM and SEM Fractography in Stress Corrosion of 4340 Steel	58
27. Comparison of TEM and SEM Fractography in Stress Corrosion of 4340 Steel	60
28. Comparison of TEM and SEM Fractography in Impact of High Speed Steel	62
29. Comparison of TEM and SEM Fractography in Impact of High Speed Steel	64
30. Comparison of TEM and SEM Fractography in Impact of High Speed Steel	66

LIST OF ILLUSTRATIONS (Concluded)

Figure	Page
31. Comparison of TEM and SEM Fractography in Impact of Plain Carbon Steel	68
32. Comparison of TEM and SEM Fractography in Impact of Plain Carbon Steel	70
33. Comparison of TEM and SEM Fractography in Impact of Plain Carbon Steel	72
34. Comparison of TEM and SEM Fractography in Impact of Low Alloy Mn Steel	74
35. Comparison of TEM and SEM Fractography in Impact of Low Alloy Mn Steel	76
36. Comparison of TEM and SEM Fractography in Overload of Ti 8-1-1 Alloy	78
37. Comparison of TEM and SEM Fractography in Overload of Ti 8-1-1 Alloy	80
38. Comparison of TEM and SEM Fractography in Overload of Ti 8-1-1 Alloy	82
39. Comparison of TEM and SEM Fractography in Fatigue of Ti 8-1-1 Alloy	84
40. Comparison of TEM and SEM Fractography in Fatigue of Ti 8-1-1 Alloy	86
41. Comparison of TEM and SEM Fractography in Fatigue of Ti 8-1-1 Alloy	88
42. Comparison of TEM and SEM Fractography in Stress Corrosion of Ti 8-1-1 Alloy	90
43. Comparison of TEM and SEM Fractography in Stress Corrosion of Ti 8-1-1 Alloy	92
44. Comparison of TEM and SEM Fractography in Stress Corrosion of Ti 8-1-1 Alloy	94
45. Comparison of TEM and SEM Fractography in Stress Corrosion of Ti 8-1-1 Alloy	96
46. Topographic Comparison of Replica and Surface	98

CHAPTER I

INTRODUCTION

Fracture surfaces of metals have been studied since the beginning of the art of metallurgy. The fracture textures indicated to the smiths and bell makers whether or not the metals they were using were suitable for the jobs they were intended. These early fracture examinations were made only with the unaided eye. Even today such examinations are still used by some metal producing companies to judge melts produced by their furnaces.

The optical microscope was first used to study fracture surfaces in 1722 by Réaumur (1). From the appearance of fractures in steels Réaumur classified different types of iron with respect to their quality. Many other good microscopic studies followed. Martins (2) described the "river patterns" characteristic of brittle fracture. Osmond, Fremont, and Gartaud (3) studied the modes of deformation and fracture of iron and mild steel. Albert Portevin (4, 5) published descriptions of experimental and service fractures with illustrated micrographs. In the 1940-1950 decade Zapffe and co-workers (6-14) obtained what are probably the best fractographs possible with the optical microscope. He and his colleagues made a detailed study of cleavage and were the first to observe striations on fatigue fracture surfaces (13)

All of the above detailed studies were limited to fairly flat fracture surfaces, such as cleavage and some fatigue failures, by the optical microscope itself. The main deterrent to high resolution in optical microscopy is the very small depth of field inherent in the microscope. For example a compound microscope using oil immersion at 1200X has 0.14μ resolution but only 0.08μ depth of field.

The introduction of the transmission electron microscope and suitable replication techniques for fracture surfaces opened the door of high resolution-large depth of field microscopy to the fractographer. The extremely short wave length associated with electrons, $.037\text{\AA}$ at 100KV accelerating potential, accounts for the high resolution while the small aperture angles necessary to reduce inherent lens aberrations give rise to a large depth of field. For example a transmission microscope set for 4,000X can show a resolution of 250\AA and have a 500μ depth of field.

Studies of many varieties of fractures have been made using the transmission electron microscope. The most notable compilations of electron fractographs are A. Phillips' Electron Fractography Handbook (15) and Henry and Plateau's La Microfractographie (16). It is demonstrated in these volumes that, although the number of alloys and conditions of fracture are vast, most fractures fall into a limited number of categories. These modes of fracture are characterized by the terms dimple rupture, cleavage, fatigue, and intergranular separation. While the appearance of a particular mode of fracture may vary from metal to metal and even from alloy to alloy

of the same metal there are enough typical similarities to allow one to transfer experience from one system to another.

The small penetration power of an electron beam makes the use of a thin film replica of a fracture surface the necessary medium for transmission studies. Many replica techniques have been devised but the one most frequently used is the two stage plastic-carbon replica. While this technique is fairly simple and does not harm the sample surface, it has its inherent undesirable aspects. Plastic replicas are often difficult to strip from rough surfaces. They are subject to many artifacts such as improper replication of small secondary cracks and air bubble encapsulation. The carbon secondary replica adds more artifacts. High ridges may collapse and the carbon film may break during dissolution of the plastic. This technique also presents the surface as a negative impression (i.e., holes appear as mounds and vice versa).

Another technique used in transmission electron fractography is that of stereoscopy. By taking two micrographs of the same area tilted at different angles to the electron beam, one can obtain a stereo pair. Although this technique aids greatly in interpretation of surface topography it is often quite difficult in observing a negative replica to properly invert ones mental picture to a proper topographical image of the surface.

The direct observations of fracture surfaces has been made practical with the recent introduction of the scanning electron microscope. This instrument is capable of low magnification (about 20X)

up to a magnification of about 20,000X which can demonstrate its resolution limit of about 150\AA . Because of its small angular aperture it also has a large depth of field (about 300 times that of an optical microscope). The imaging process of the scanning electron microscope, which will be discussed later, gives a picture of the surface with such realistic topographical perceptibility that even the novice or layman can relate to them. The sample preparation simply entails cutting the sample to a certain size. All of the artifacts introduced by replication are of course eliminated.

Many metallurgists have found difficulty in translating their experience with transmission fractography to the new look afforded by the scanning electron microscope. Some of the typical features one has grown accustomed to seeing by replication aren't at first glance as apparent in the SEM. There has not yet been published any large atlas or handbook of scanning electron fractographs, although there are at least two in the making but a few papers have been published dealing with the comparison of TEM and SEM fractography. These articles have shown TEM and SEM micrographs of the typical features of the different modes of fracture but a one to one correspondence is still lacking.

The purpose of this work is to prepare an atlas giving this one to one comparison of transmission and scanning electron fractography. Transmission micrographs using the plastic-carbon replica technique and scanning micrographs have been taken from a variety of samples and fracture modes. Each transmission micrograph, taken

and presented here in stereo, is accompanied by a stereo scanning electron micrograph of the identical area and at the same magnification. Another scanning micrograph of this area at some oblique angle to it is also presented. A study of these comparisons will familiarize the fractographer with what he should expect to see in scanning electron micrographs as compared to what he is due to seeing in his transmission fractographs.

CHAPTER II

INSTRUMENTATION AND EQUIPMENT

Transmission Electron Microscope

Figure 1 is a schematic representation of an electron microscope. Electrons produced at the source are accelerated down the evacuated microscope column, by a high potential, usually 40 to 100 kilovolts. These electrons are affected by the magnetic fields produced by the electromagnetic lens in a similar manner as light is affected by the glass lenses in an optical microscope. The condenser lens focuses the electron beam onto the sample. An enlarged image of the sample is formed by the objective lens. This image is further enlarged and projected onto the fluorescent viewing screen by the projector lens. Magnification and focus are controlled by varying the currents through the projector and objective lenses.

As electrons pass through the replica some are scattered by interaction with the replica. The number of electrons scattered is dependent in part on the thickness of the replica. These scattered electrons are removed from the beam by a small aperture below the sample and do not contribute to the formation of an image. Therefore thicker parts of the replica appear darker in the final image.

The microscope used in this study was a Philips EM 200. This microscope is equipped with a device which will tilt the replica 6° to either side of center for the taking of stereo pairs of micrographs.

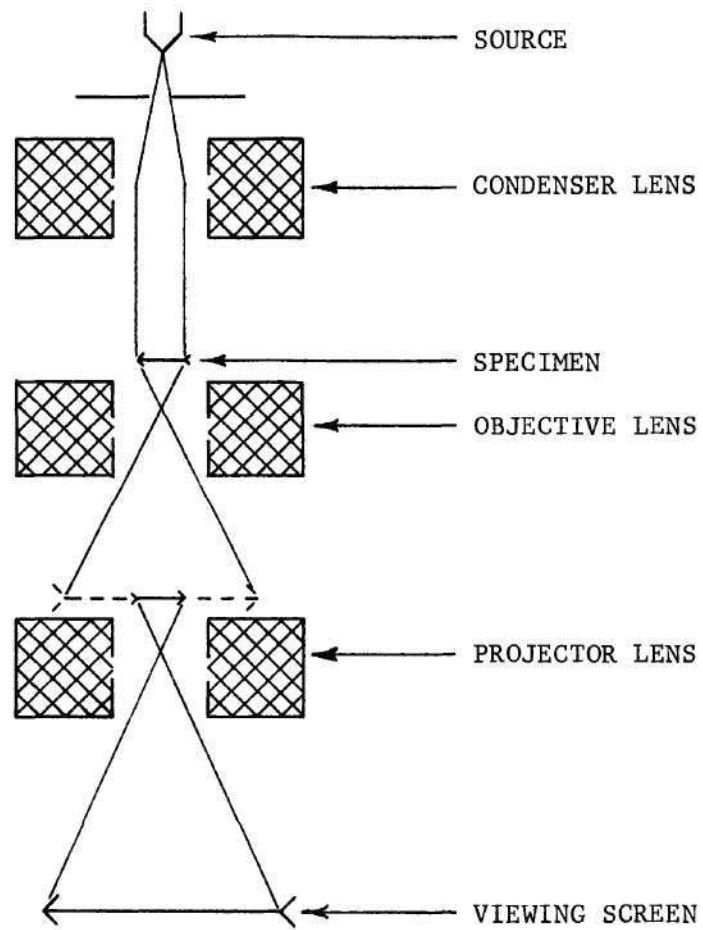


Figure 1. Schematic Drawing of a Transmission Electron Microscope

A 35mm camera is positioned in the column between the projector lens and the viewing screen and may be moved into the beam to record the image.

Scanning Electron Microscope

Figure 2 is a schematic representation of a scanning electron microscope. As in the transmission microscope electrons from the source are accelerated down the evacuated column and controlled by the magnetic fields of the lenses. The sample to be viewed is at the bottom of the column and the lenses are set so that a point image of the source is focused on the specimen. This electron probe striking the sample, causes the emission of various signals by the sample. These are secondary electrons, backscattered electrons, x-rays, sample current, and possibly cathodoluminescence. One of the strongest and most used signals is that of the secondary electrons.

Secondary electrons have a relatively low energy and therefore can be easily collected. Figure 3 is a diagram of the collector system. The front screen is kept at a positive potential of 250 volts. The scintillator is a hemispherical piece of plastic in which is embedded an organic scintillation material. This piece is glued to the end of a lucite rod and is coated with a thin aluminum film which is kept at a positive potential of 12,000 volts. The secondary electrons emitted from the sample are drawn to the front screen of the collector and then accelerated toward and into the scintillator. The scintillator produces light from the electron bombardment which it transmits through the lucite rod to a photomultiplier tube.

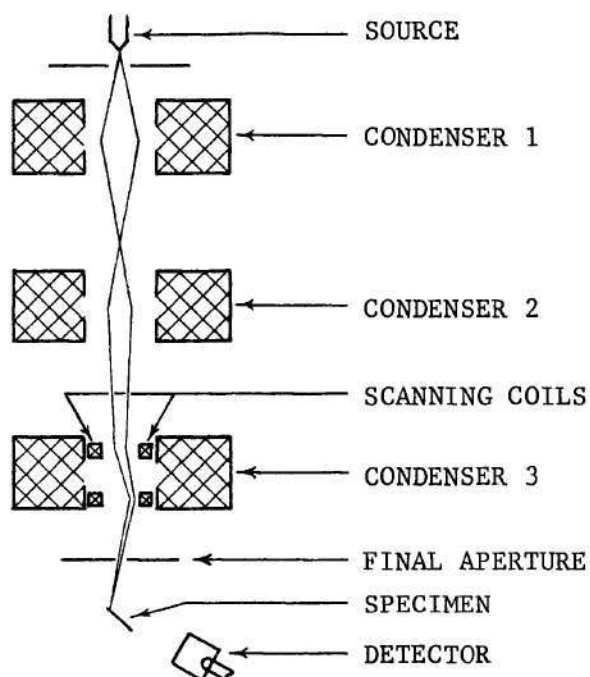


Figure 2. Schematic Drawing of a Scanning Electron Microscope

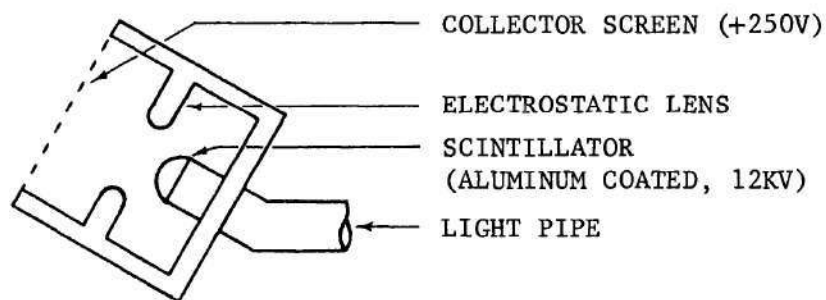


Figure 3. Diagram of a Secondary Electron Collector from a Scanning Electron Microscope

The electron probe is caused to scan the surface of the sample in a raster pattern. The electron beam of a cathode ray tube is synchronized to raster with the scanning electron probe and the intensity of the beam controlled by the signal received from the probe-stimulated secondary electron emission. In this way a picture of the surface is drawn on the cathode ray tube. Focusing is obtained by controlling the lens currents to give an appropriate size probe diameter on the sample. The magnification is changed by changing the area scanned by the probe.

The scanning electron microscope used in this study was the Cambridge Stereoscan Mark II. The stage on this microscope allows the sample to be moved in three orthogonal directions, rotated 360° , and tilted from a position normal to the electron probe to a position 90° from this and facing the collector.

At the beginning of this study stereo pairs of micrographs were made by tilting the sample through 12° using the normal stage controls. To view these micrographs in stereo it was necessary to rotate the picture 90° from their normal viewing direction. Figure 7 is one example of a stereo made in this manner. Since this detracted from the perspective of the picture it was necessary to construct a special stereo adapter for the stage. Figure 4 is a picture of this adapter. Part A is a blank holder whose top surface has been cut 6° off from its normal plain. This piece fits in the normal sample stub position in the stage. Part B is a thin disc of aluminum with a diametrical slot across the top surface. The sample is attached to

this piece which sits atop part A and is held in position by the tungsten springs of part C. Part C is a blank test sample holder to which a tungsten spring has been attached and which is placed in the normal test sample position. Figure 5 shows these parts in their proper positions on the microscope stage. Using the stage rotation control part A can be rotated under part B giving a tilt of 6° to either side of center to the sample. Stereo micrographs made using this attachment can be viewed without rotation of the picture thereby retaining proper perspective. Figure 13 is an example of a stereo made using this attachment.

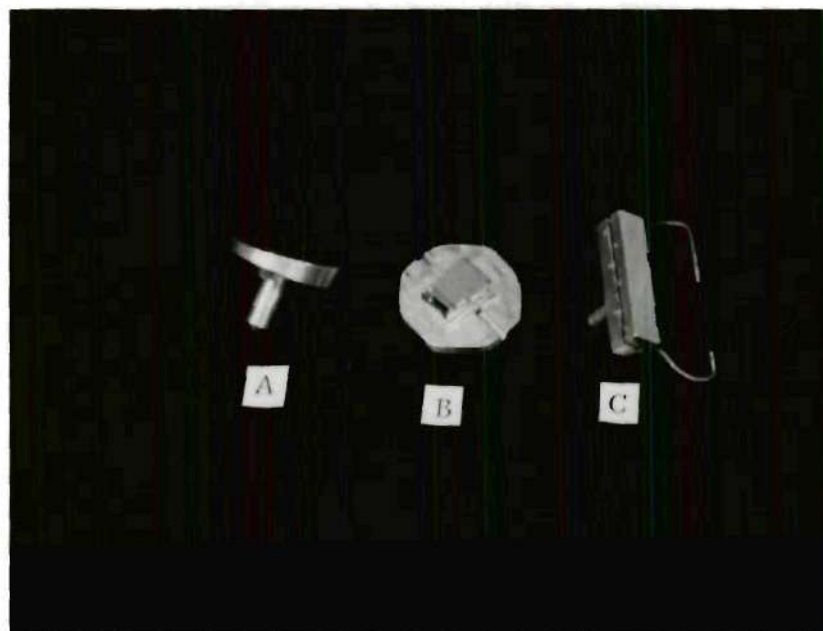


Figure 4. Stereo Adapter Parts for the SEM Stage

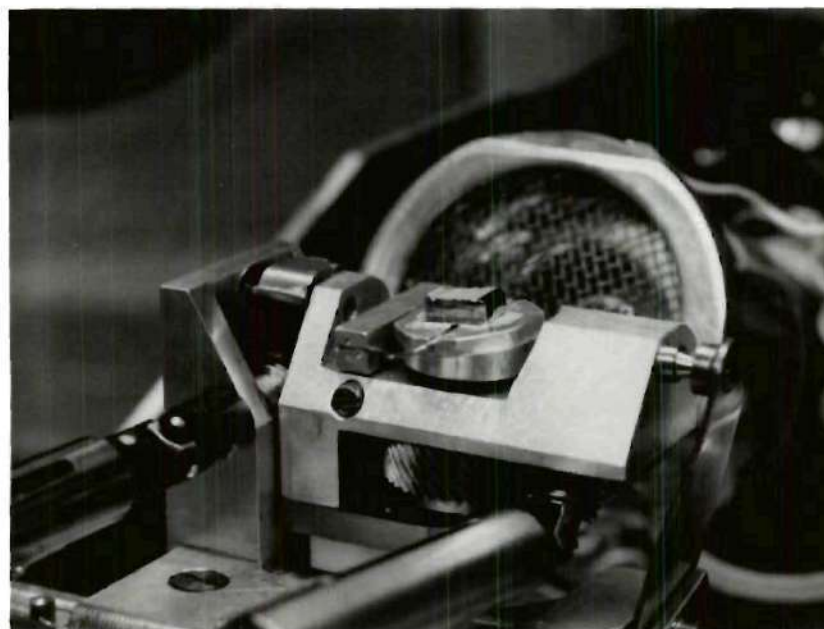


Figure 5. Stereo Adapter in Its Proper Position on the SEM Stage

CHAPTER III

PROCEDURE

Sample Marking

The samples used in this study were obtained from a number of sources. Some were test specimens made for the purpose of fracture studies and some were service type failures. By means of a low power optical stereo microscope an appropriate area was selected for study. A small scratch was made in the center of this area with a steel or diamond stylus to give a reference mark to be used in identifying the areas studied.

Replication

A replica was made of each marked area using Fullam replica tape #1134. This tape was placed in acetone and allowed to soften to a point of just becoming limp. It was then placed on the marked area of the fracture and pressed to remove air bubbles and replicate crevices. The tape was allowed to harden in place and was then stripped from the fracture surface. This first plastic replica was made to clean the fracture surface and was discarded. The process was then repeated to obtain a replica of each cleaned surface.

The replicas were placed in a vacuum evaporator, Kinney model KDTG-3P, equipped with a carbon evaporator and a tungsten filament onto which had been wrapped a 12mm length of 10 mil diameter

platinum wire. The tungsten filament was placed 10cm from the replicas and 45° to the replica surfaces. The carbon rods to be evaporated were also 10cm from the replicas but directly over them. The pressure in the vacuum bell jar was reduced to at least 10^{-4} torr. A current was passed through the tungsten filament, heating it sufficiently to melt and evaporate the platinum which coated the replicas. Protuding features on the replicas caught the platinum and shaded adjacent areas behind them. This gives a shadowing effect to the replica which aids in topographical perception. The carbon was evaporated from directly above the replicas and coated the entire surface of the replica. The thickness of the platinum shadowing was about 20-30Å and that of the carbon about 100Å.

The index scratches were located on the platinum shadowed-carbon coated replicas and acute equilateral triangular pieces containing the scratches cut from them. The apex of each triangle was cut to point in some particular direction with respect to the original sample. Each replica was placed, platinum-carbon side down, on a 150 mesh copper electron microscope grid, which was sitting on a copper screen bridge in a small petri dish. The dish was filled with acetone to the level of the bridge, covered, and left for an hour or more. The acetone dissolved the plastic leaving only the platinum-carbon replica on the grid. The acetone was siphoned from the petri dish and the grid picked up with a pair of fine tipped tweezers. A piece of filter paper was touched to the grid drawing off all remaining acetone. The replicas were now ready for viewing in the microscope.

Transmission Electron Microscopy

Each grid was placed in the electron microscope sample holder with care to position the apex of the replica triangle in the direction of the axis around which the holder is rotated to obtain stereo pairs. The replica was scanned at low power in order to locate the index scratch. Stereo micrographs were taken of typical areas near the scratch but far enough away to be unaffected by it. The angle of tilt used for stereo was $\pm 6^\circ$ on either side of the normal position. Low power micrographs were taken of these and surrounding areas including the scratched areas. Prints were made of these micrographs before the scanning electron microscopy was done.

Scanning Electron Microscopy

The areas containing the scratches were cut from the samples and individually mounted on the slotted plate of the scanning microscope stereo holder. The direction of the sample used to index the triangular replica piece was aligned with the slot and thereby with the axis of tilt used for stereo microscopy. The areas of interest were first located by scanning at low magnification and comparing with the low magnification transmission micrographic prints. The exact areas of which micrographs were taken of the replicas were located and the magnification set to the same figure as each respective transmission micrograph. A stereo pair of scanning electron micrographs was made of each area with the fracture surface tilted 6° on both sides of a position normal to the electron probe. The sample was then tilted to some oblique angle and a single micrograph made.

Stereoscopy

By measuring the parallax between points on the stereo micrographs the differences in the height of these points can be calculated. Figure 6 is a representation of two points, A and B, on the surface of a replica in its normal position. The points B' and B'' represent the new positions of B relative to A after the replica has been tilted through the angle θ on both sides of the normal position. D is the straight line distance between points A and B, γ is the angle this line makes with the plane which is parallel to the general replica plane and contains point A, and Δh is the height of point B above this plane. X is the projected distance between A and B as seen on the micrograph of the replica tilted through the angle θ in one direction, while $X+\Delta X$ is the projected distance between A and B as seen on the micrograph of the replica tilted through the angle θ in the opposite direction. From Figure 6 it can be seen that

$$\sin \gamma = \frac{\Delta h}{D}; \quad (3-1)$$

$$\cos (\gamma+\theta) = \frac{X}{D}; \quad (3-2)$$

$$\text{and} \quad \cos (\gamma-\theta) = \frac{X+\Delta X}{D} \quad (3-3)$$

From trigonometric identities:

$$\cos (\gamma+\theta) = \cos \gamma \cos \theta - \sin \gamma \sin \theta = \frac{X}{D} \quad (3-4)$$

$$\cos (\gamma-\theta) = \cos \gamma \cos \theta + \sin \gamma \sin \theta = \frac{X+\Delta X}{D} \quad (3-5)$$

Subtracting equation (3-4) from (3-5) gives

$$\sin \gamma \sin \theta + \sin \theta = \frac{X + \Delta X}{D} - \frac{X}{D}$$

$$\text{or} \quad 2 \sin \gamma \sin \theta = \frac{\Delta X}{D} \quad (3-6)$$

Substituting equation (3-1) into (3-6) gives

$$2 \frac{\Delta h}{D} \sin \theta = \frac{\Delta X}{D}$$

$$\text{or} \quad 2 \Delta h \sin \theta = \Delta X \quad (3-7)$$

Where the actual distances measured have been magnified by some factor M, as in the electron micrographs, the formula would be.

$$2M\Delta h \sin \theta = \Delta X \quad (3-8)$$

Measurements were made for a number of points along identical lines in the transmission and scanning electron micrographs of the area seen in Figure 7. ΔX was measured using a Wild Heerbrugg parallax bar and Δh calculated using equation (3-8). The results of these measurements are given in Chapter V.

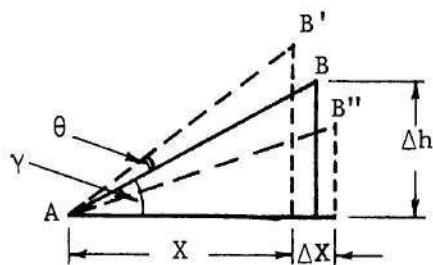


Figure 6. Relative Positions of Two Points Before and After Tilting Through + and - the Angle θ .

CHAPTER IV

COMPARISON ATLAS

Figure 7 through 46 are comparisons of transmission and scanning electron fractographs. The page preceeding each figure gives the information pertinent to the material and the micrographs. A comparison of some of the features seen on the micrographs is also presented on this page.

On each figure a stereo pair of transmission electron micrographs is presented at the top of the page, a stereo pair of scanning electron micrographs in the center, and a single scanning electron micrograph at the bottom. The single scanning micrograph was made at some angle other than normal to the fracture surface. Both the transmission and the scanning micrographs are of the same area of the sample.

The materials used in this study were 7075 Al alloy, 4340 steel, high speed steel, plain carbon steel, low alloy Mn steel, and Ti 8-1-1 alloy. The modes of fracture studied were overload, fatigue, stress corrosion, and impact.

Figure 7. Comparison of TEM and SEM Fractography in Overload of Al Alloy (on following page)

Material: Aluminum 7075

Heat Treatment: T6

Type of Test: Overload; notched-tension; strain rate of $0.002 \text{ in}^2/\text{min}$.

Ultimate Strength: 85,900 psi

Test Environment: Air at ambient temperature

Magnification of Fractographs: 2500X

Tilt of Single Scanning Micrograph: 30°

Appearance of Fracture: The fracture consists primarily of fine dimples and second phase particles.

Comparison Analysis: The center portion of the second phase particle at the top center of the transmission micrograph appears to be in approximately the same plane as the dimpled region and surrounded by a trench. The dark area around the second phase particle at the lower left is due to an overlapping carbon replica film. The scanning micrograph shows that the second phase particle at the top center rises appreciably above the surface of the dimple area. This area should have appeared as a deep hole in the transmission micrograph but it is apparent that this feature was too high for the replica to stand up and the sloping wall folded forming the apparent trench. The true topography of the bottom left feature is very apparent.

One can get a good idea of these topographical features from the single tilted scanning micrograph without the use of stereo. The orientation of this picture is turned 90° clockwise from that of the stereo pair.

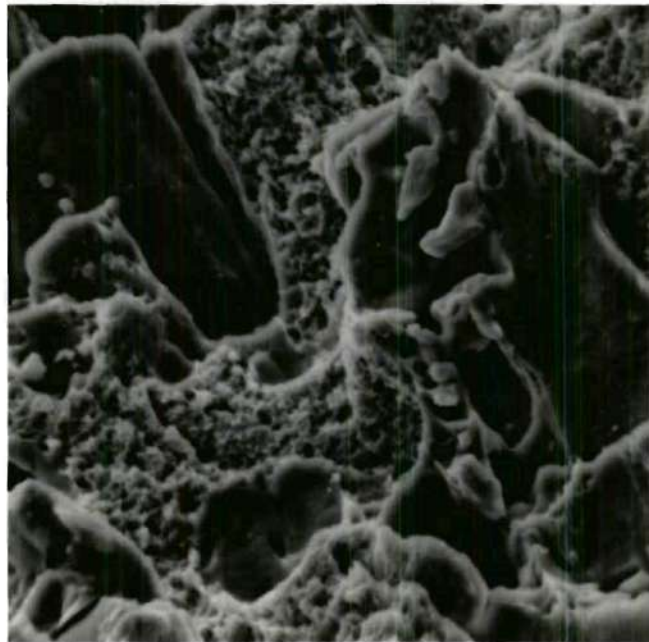
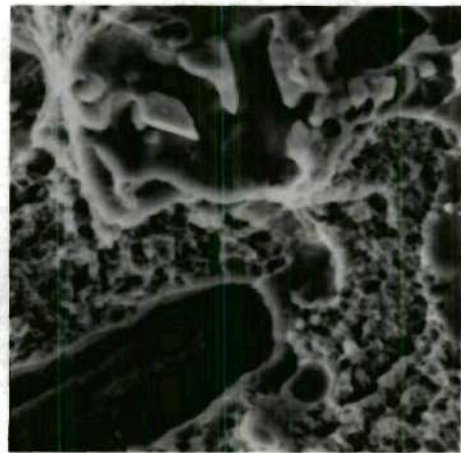
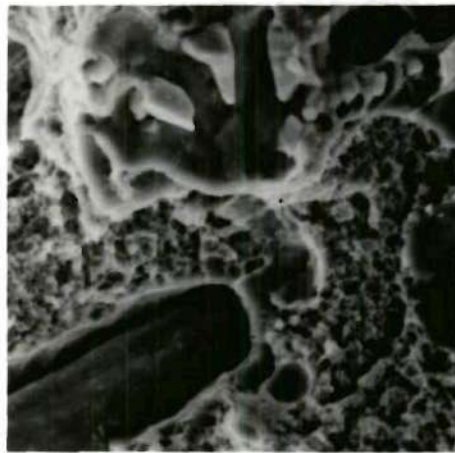
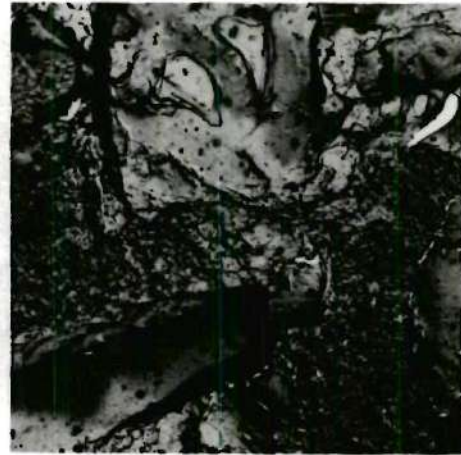


Figure 8. Comparison of TEM and SEM Fractography in Overload of Al Alloy (on following page)

Material: Aluminum 7075

Heat Treatment: T6

Type of Test: Overload; notched-tension; strain rate of $0.002 \frac{\text{in}}{\text{min}}$.

Ultimate Strength: 85,900 psi

Test Environment: Air at ambient temperature

Magnification of Fractographs: 5250X

Tilt of Single Scanning Micrograph: 40°

Appearance of Fracture: The fracture consists primarily of fine dimples and second phase particles.

Comparison Analysis: In the transmission micrograph the ends of some of the shear dimples on the left stick up in peaks due to some stretching of the plastic replica as it is pulled from the surface. The protrusion to the right of the spherical feature is undoubtedly due to a hole but its proper inverted interpretation is difficult. The dark spots are artifacts probably due to the deposition of some foreign material during dissolution of the plastic. The true topography is easily seen in the scanning micrograph however the lower resolution is shown by the lack of the fine detail seen on the sheer dimples in the transmission micrograph.

The single scanning micrograph shows the topography very well without the use of stereo although the deep hole beside the spherical particle is hidden. The orientation of this picture is turned 90° clockwise from that of the stereo pair.

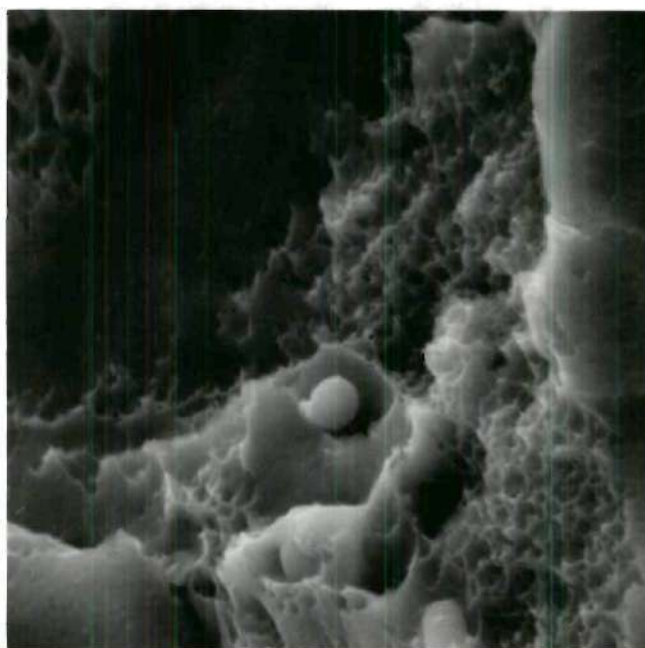
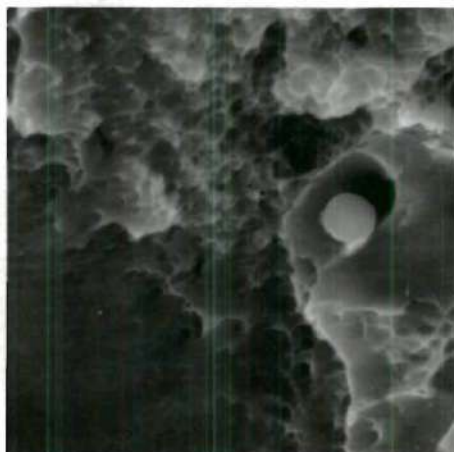
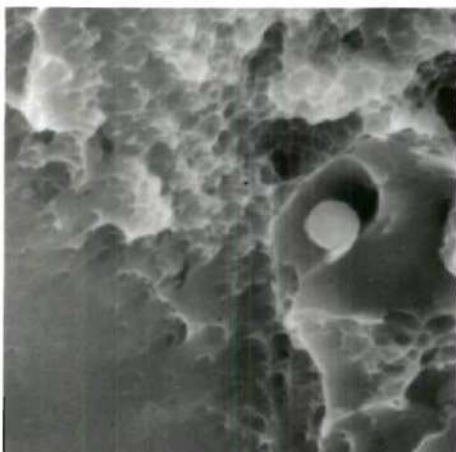
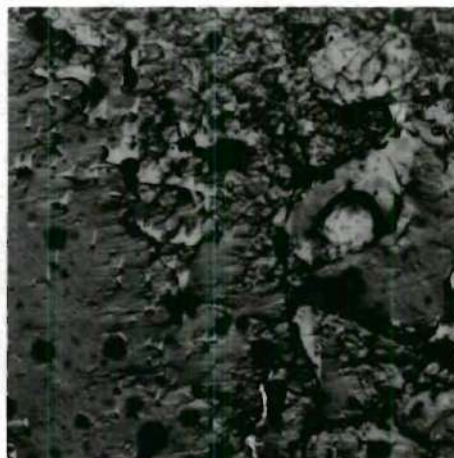
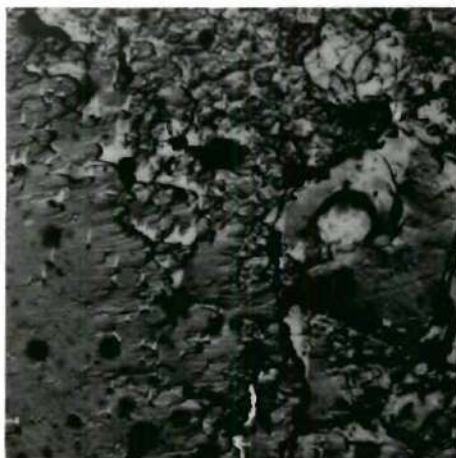


Figure 9. Comparison of TEM and SEM Fractography in Overload of Al Alloy (on following page)

Material: Aluminum 7075

Heat Treatment: T6

Type of Test: Overload; notched-tension; strain rate of $0.5 \text{ in}^n/\text{min.}$

Ultimate Strength: 68,100 psi

Test Environment: Air at ambient temperature

Magnification of Fractographs: 2520X

Tilt of Single Scanning Micrograph: 45°

Appearance of Fracture: The fracture consists primarily of fine dimples and second phase particles.

Comparison Analysis: In the transmission micrograph the three general areas shown, (bottom left, center, and top right) all appear to be on about the same level. The center and top right portions are separated by a dark band. This band is an artifact caused by tearing and overlapping of the carbon replica. The scanning micrograph shows these three areas to actually be on quite different levels. Note that the tearing of the replica occurred at a place where the elevation was changing very rapidly.

The single scanning micrograph reveals this topography to some extent without the use of stereo. Besides its tilt, the orientation of this picture is turned 90° clockwise from that of the stereo pair.

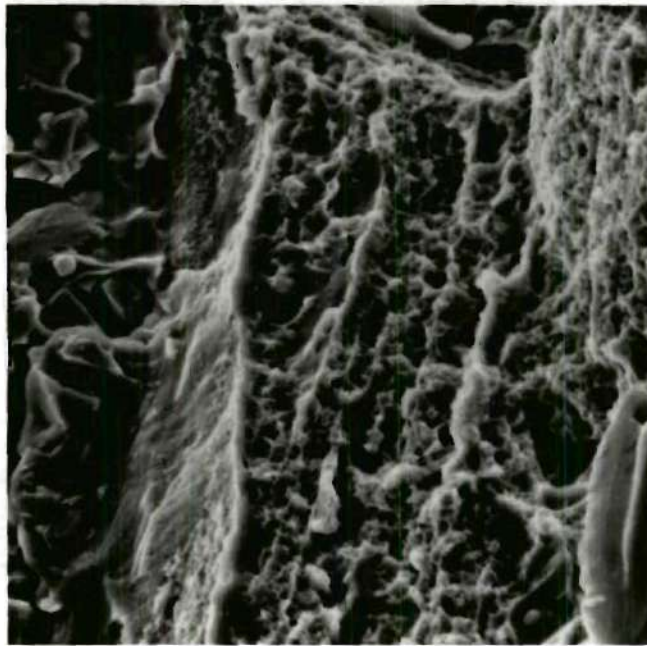
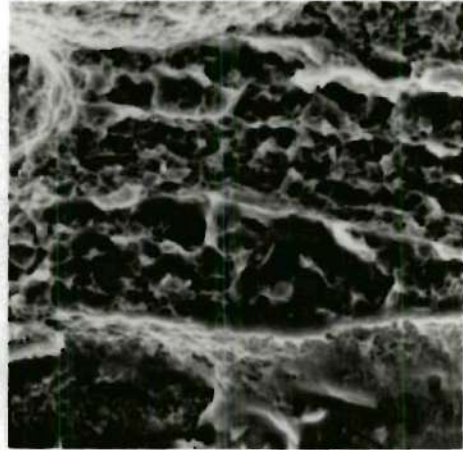
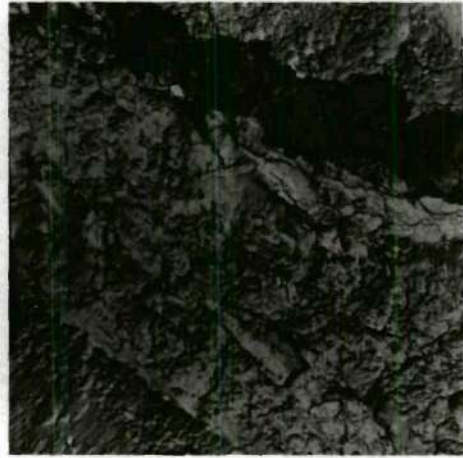


Figure 10. Comparison of TEM and SEM Fractography in Overload of Al Alloy (on following page)

Material: Aluminum 7075

Heat Treatment: T6

Type of Test: Overload; notched-tension; strain rate of $0.5 \text{ in}^n/\text{min}$.

Ultimate Strength: 68,100 psi

Test Environment: Air at ambient temperature

Magnification of Fractographs: 4200X

Tilt of Single Scanning Micrograph: 45°

Appearance of Fracture: The fracture consists of fine dimples and secondary particles.

Comparison Analysis: The transmission and scanning micrographs are in very good register in this comparison. At this magnification one can easily see the finer detail afforded by the shadow enhancement and higher resolution of the transmission microscope.

The single tilted scanning micrograph gives a better idea of surface topography than does the stereo. The orientation of this picture, besides its tilt is turned 90° clockwise from that of the stereo.

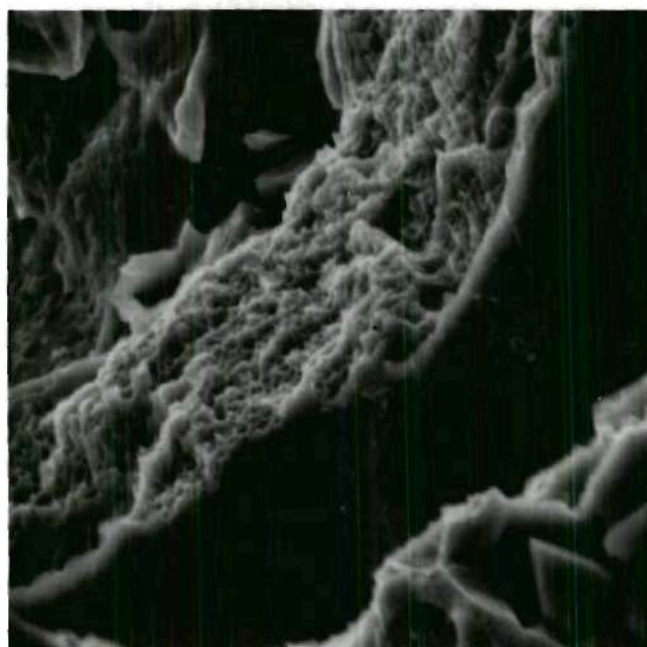
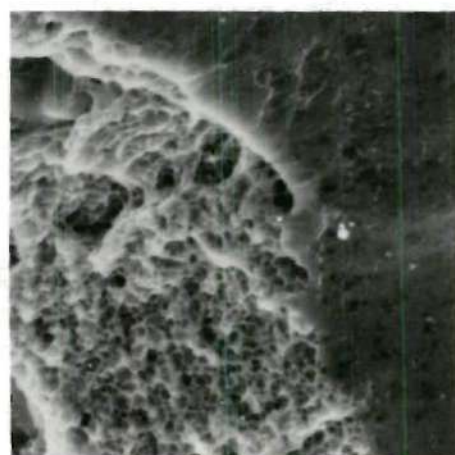
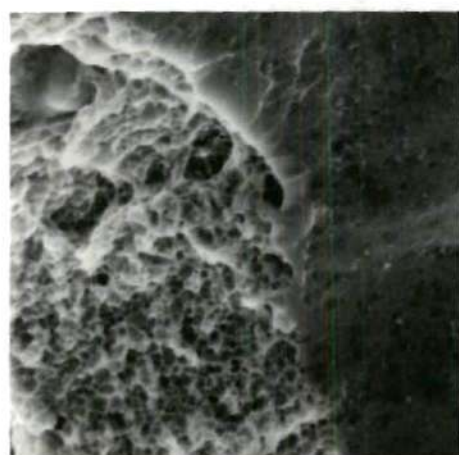
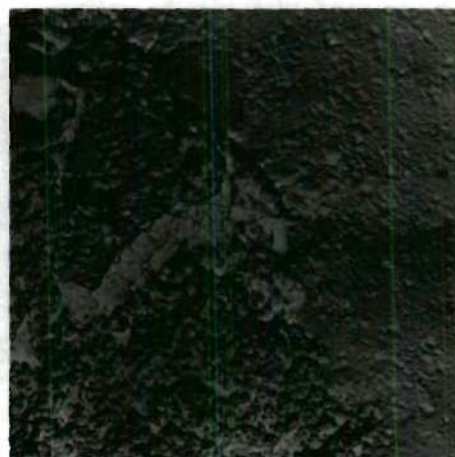
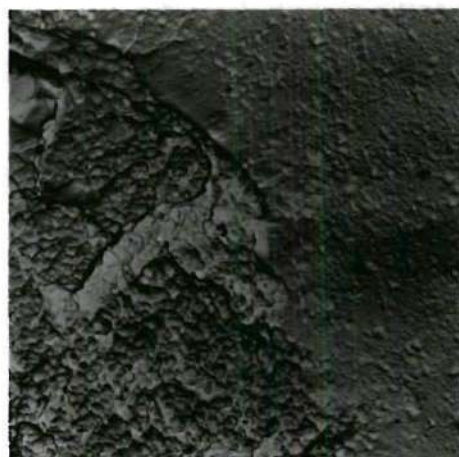


Figure 11. Comparison of TEM and SEM Fractography in Overload of Al Alloy (on following page)

Material: Aluminum 7075

Heat Treatment: T6

Type of Test: Overload; notched-tension; strain rate of 400 ⁱⁿ/min.

Ultimate Strength: 68,200 psi

Test Environment: Air at ambient temperature

Magnification of Fractographs: 2000X

Tilt of Single Scanning Micrograph: 40°

Appearance of Fracture: The fracture consists of fine dimples, secondary particles and some stretched areas.

Comparison Analysis: The transmission micrograph indicates the surface is fairly flat however there are many indications of collapse of the replica. Torn, overlapped, and folded areas are seen in a number of places on the replica. There are also some long stringy bits of carbon replica from some other broken areas lying on this one. The scanning micrograph shows that the area is quite rough. This comparison is representative of the most severe replica collapse encountered in this study.

The single scanning micrograph reveals the topography very nicely without the use of stereo. The orientation of this picture is turned 90° clockwise from that of the stereo.

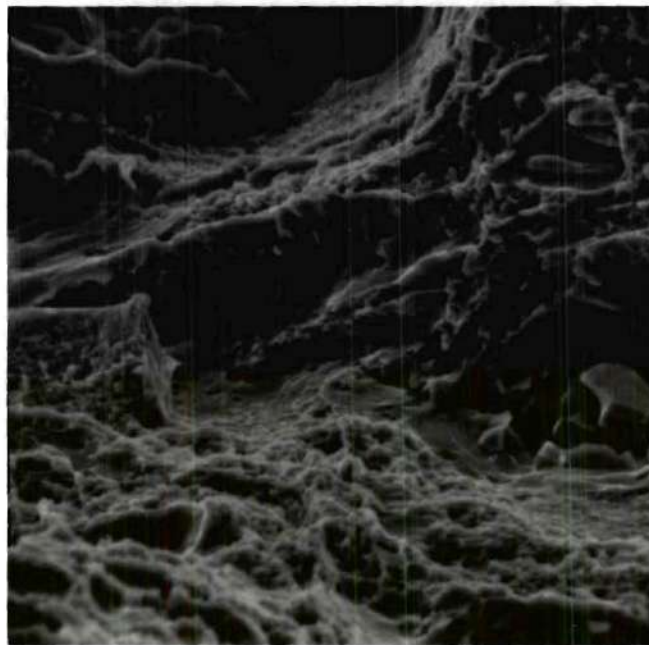
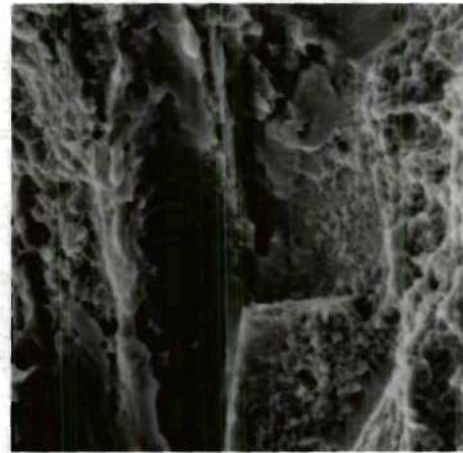
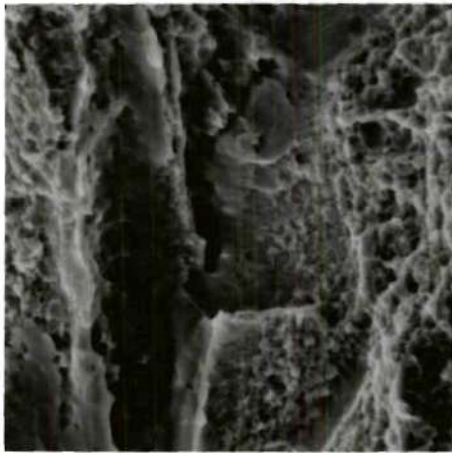


Figure 12. Comparison of TEM and SEM Fractography in Overload of Al Alloy (on following page)

Material: Aluminum 7075

Heat Treatment: T6

Type of Test: Overload; notched-tension; strain rate of 400 ⁱⁿ/min.

Ultimate Strength: 68,200 psi

Test Environment: Air at ambient temperature

Magnification of Fractographs: 4900X

Tilt of Single Scanning Micrographs: 45°

Appearance of Fracture: The fracture consists of fine dimples and secondary particles.

Comparison Analysis: The transmission micrograph indicates the surface is fairly flat. The dimples are clearly defined. The darker area near the center with the small bubble-like formation is an artifact due to a thin film of undissolved plastic. The scanning micrograph shows the true rough topography of the surface. The dimples are not as sharply defined due to the lower resolution.

The single scanning micrograph does not reveal the surface topography too well without the use of stereo. The orientation of this picture is turned 90° clockwise from that of the stereo.

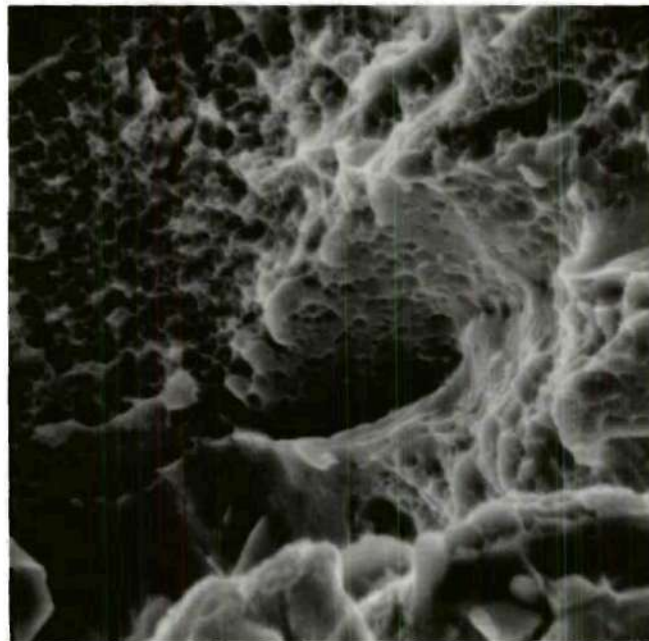
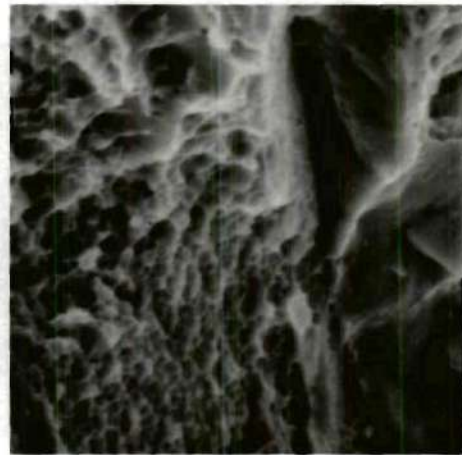
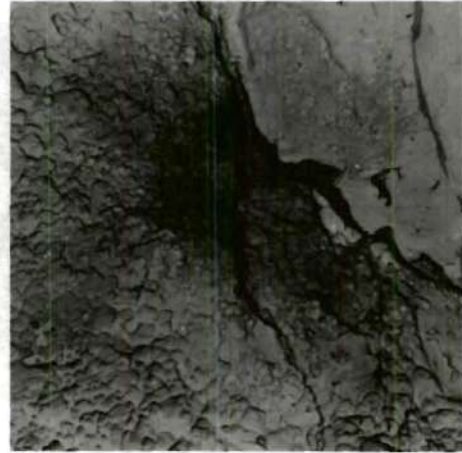
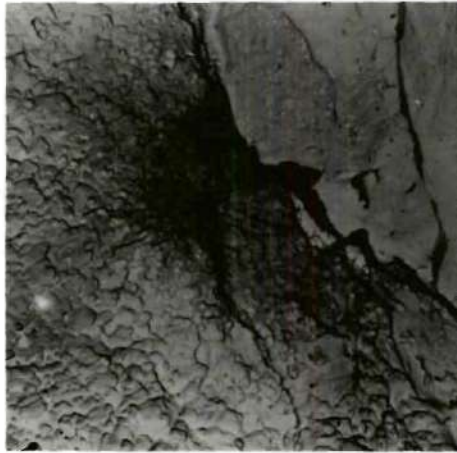


Figure 13. Comparison of TEM and SEM Fractography in Fatigue of Al Alloy (on following page)

Material: Aluminum 7075

Heat Treatment: T6

Type of Test: Fatigue; low cycle; 1900 cycles/min. at 17,000 psi max.

Ultimate Strength: 85,000 psi typical

Test Environment: Air at ambient temperature

Magnification of Fractographs: 1760X

Tilt of Single Scanning Micrograph: 30°

Appearance of Fracture: The fracture surface shows well defined fatigue striations.

Comparison Analysis: The transmission micrograph shows the fatigue striations with excellent detail and contrast. The dark areas on the right are due to folding and an apparently collapsed replica film. The scanning micrograph reveals the depth and sheer walls associated with the right portion of this view which gave rise to the collapse of this portion of the replica. The striations are not as well seen due to the lack of contrast.

The single tilted scanning micrograph shows the topography well without the use of stereo.

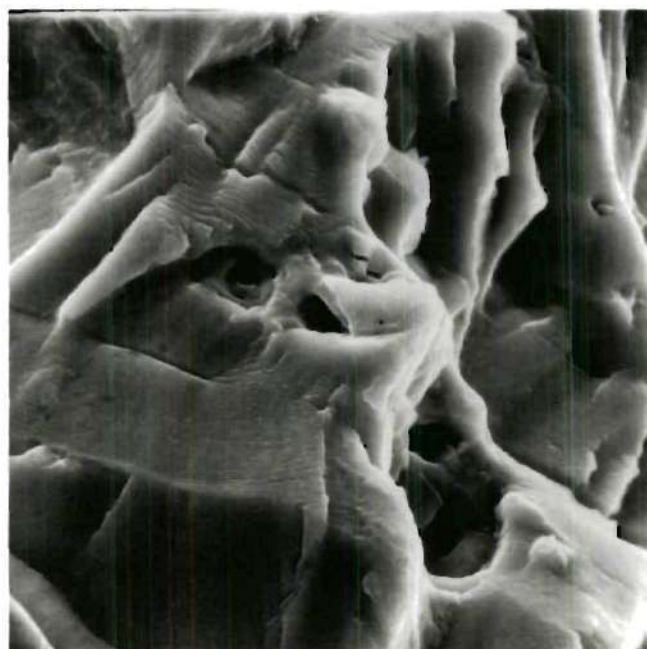
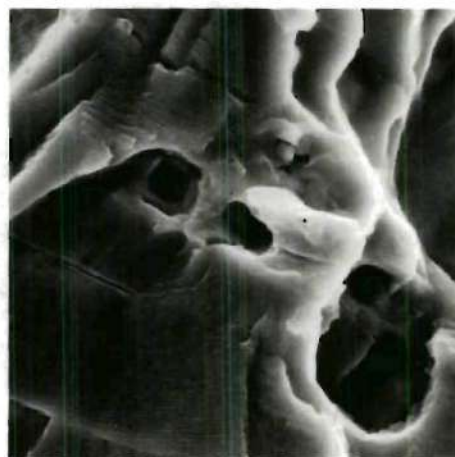
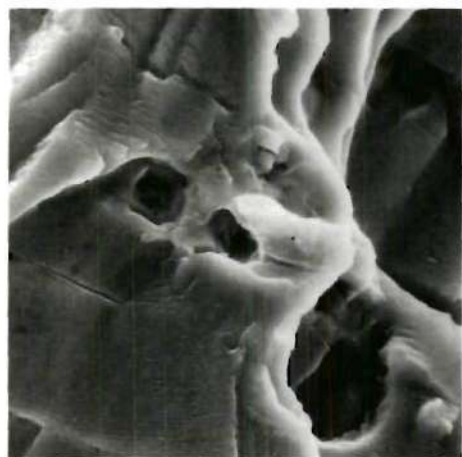
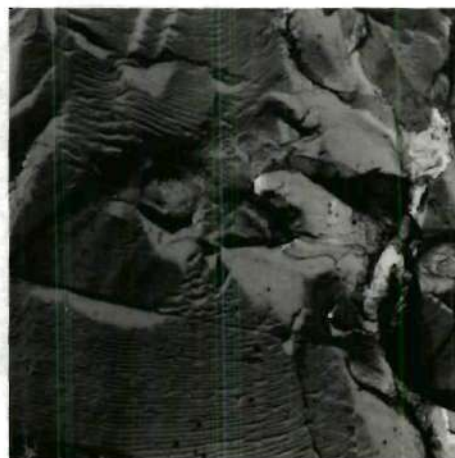


Figure 14. Comparison of TEM and SEM Fractography in Fatigue of Al Alloy (on following page)

Material: Aluminum 7075

Heat Treatment: T6

Type of Test: Fatigue; low cycle; 1900 cycles/min. at 17,000 psi max.

Ultimate Strength: 85,000 psi typical

Test Environment: Air at ambient temperature

Magnification of Fractographs: 6400X

Tilt of Single Scanning Micrograph: 30°

Appearance of Fracture: The fracture surface shows well defined fatigue striations.

Comparison Analysis: The transmission micrograph shows the fatigue striations with excellent detail and contrast. It also shows that the line running from the upper right to lower left is caused by the meeting of the planes of striations on the left and right which are at different levels. The scanning micrograph shows that the replica is in excellent correlation with the true surface. The striations are not as sharply seen but the difference in levels of the left and right sides are seen more clearly. The occasional overlap of the upper level over the lower which is not clearly shown in the transmission micrographs is very obvious in the scanning micrograph.

The single scanning micrograph does not particularly show this topography well without the use of stereo.

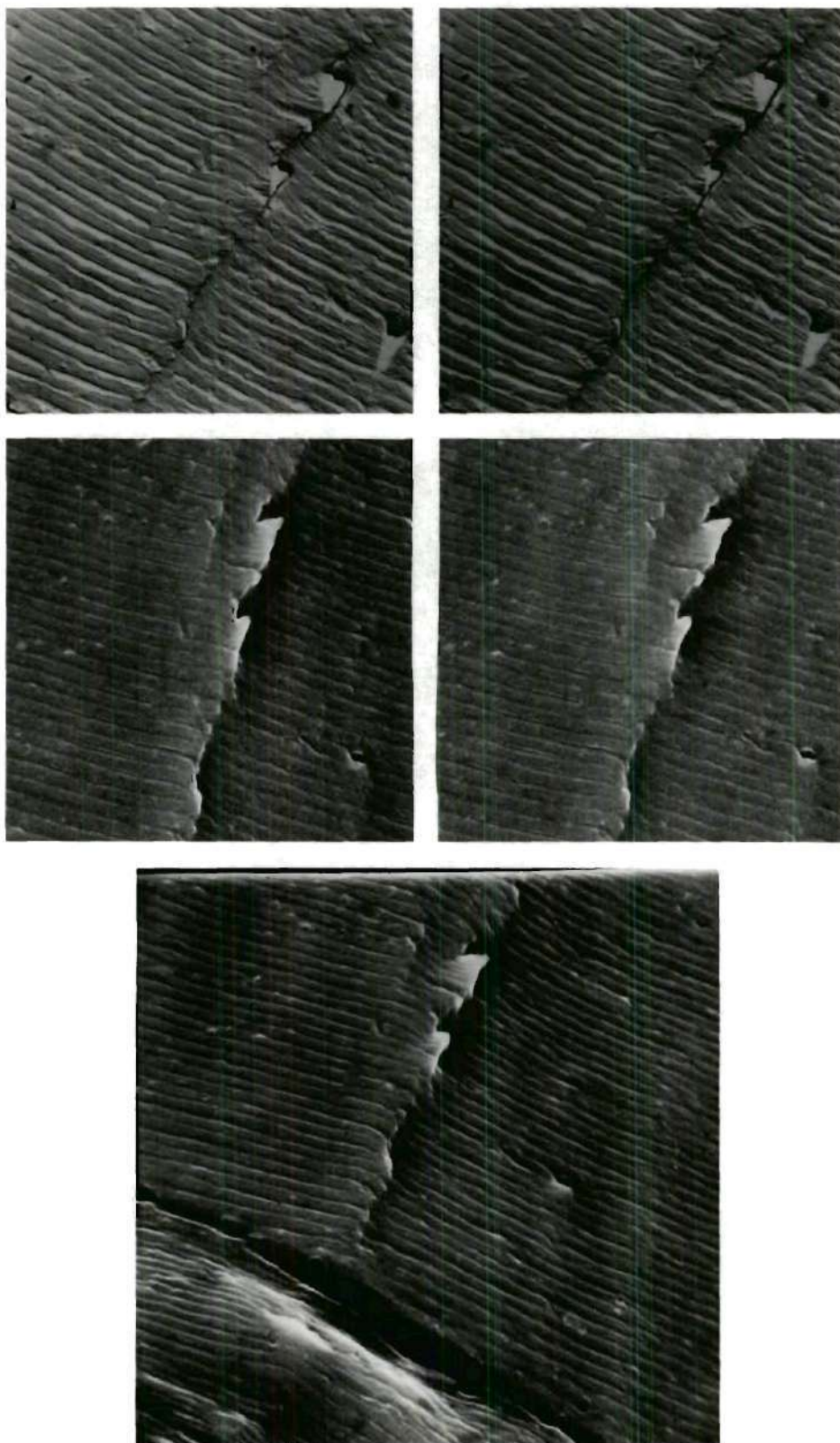


Figure 15. Comparison of TEM and SEM Fractography in Fatigue of Al Alloy (on following page)

Material: Aluminum 7075

Heat Treatment: T6

Type of Test: Fatigue; low cycle; 1900 cycles/min. at 17,000 psi max.

Ultimate Strength: 85,000 psi typical

Test Environment: Air at ambient temperature

Magnification of Fractographs: 3100X

Tilt of Single Scanning Micrograph: 30°

Appearance of Fracture: The fracture surface shows well defined fatigue striations.

Comparison Analysis: The transmission micrograph shows the striations with excellent detail and contrast. The replica is torn and overlapped in one area and some peaks of replica film indicate holes or cracks in this area. The scanning micrograph presents the true topography well. The changes from one plane to another are seen to be much sharper and with a greater angular change than indicated by the transmission micrograph. The striations are well resolved but are not as contrasty as in the transmission micrograph.

The single tilted scanning micrograph shows the topography fairly well without the use of stereo.

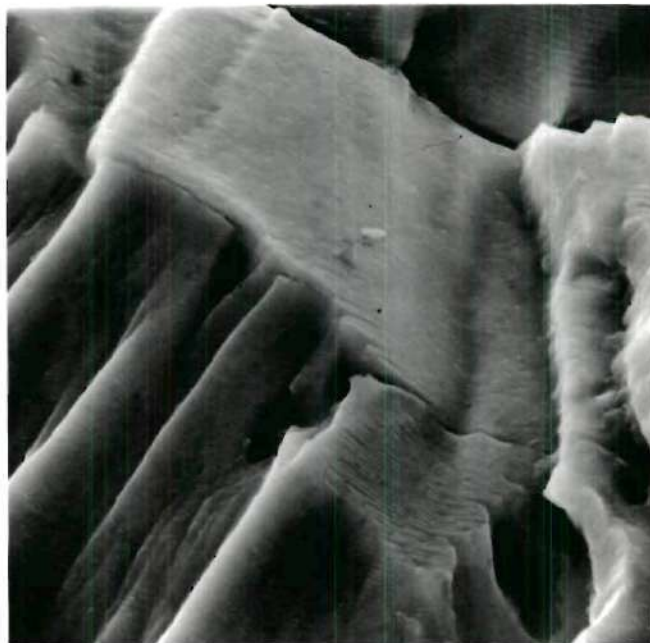
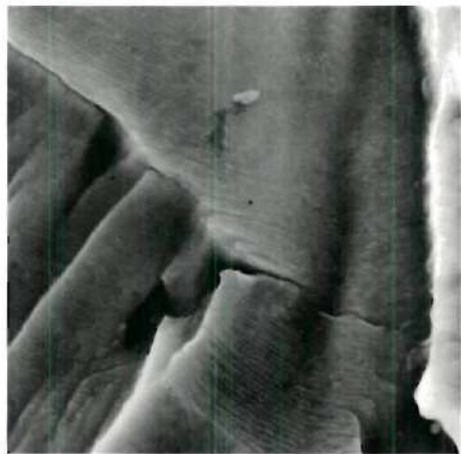
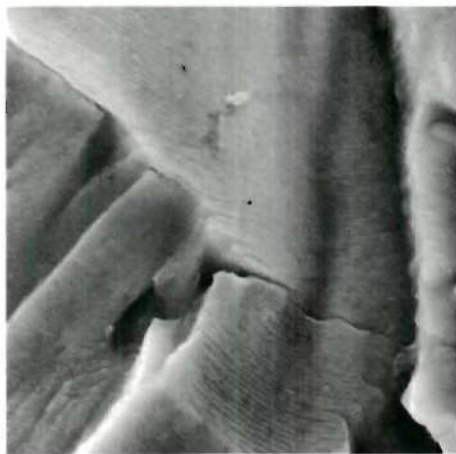
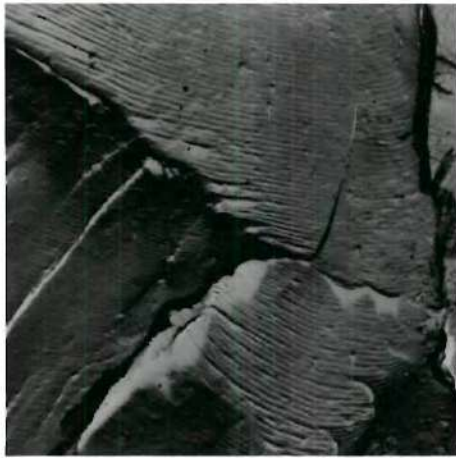


Figure 16. Comparison of TEM and SEM Fractography in Fatigue of Al Alloy (on following page)

Material: Aluminum 7075

Heat Treatment: T6

Type of Test: Fatigue; low cycle; 1900 cycles/min. at 17,000 psi max.

Ultimate Strength: 85,000 psi typical

Test Environment: Air at ambient temperature

Magnification of Fractographs: 4000X

Tilt of Single Scanning Micrograph: 30°

Appearance of Fracture: The fracture surface shows well defined fatigue striations.

Comparison Analysis: The transmission micrograph reveals the striations with excellent detail and contrast. The match between the replica and the true surface in this area is excellent. The scanning micrograph shows the striations well resolved but lacking in contrast.

The single tilted scanning micrograph shows the topography fairly well without the use of stereo.

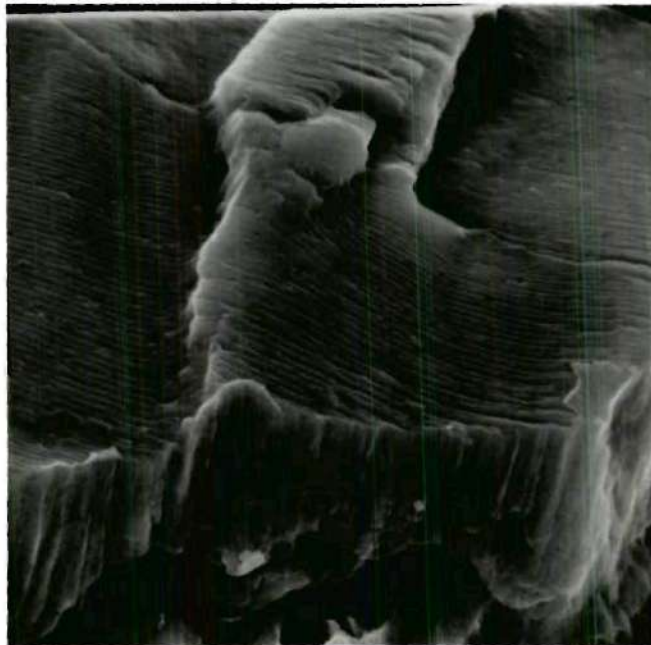
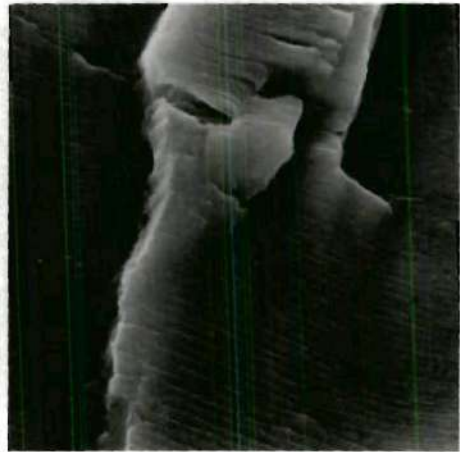
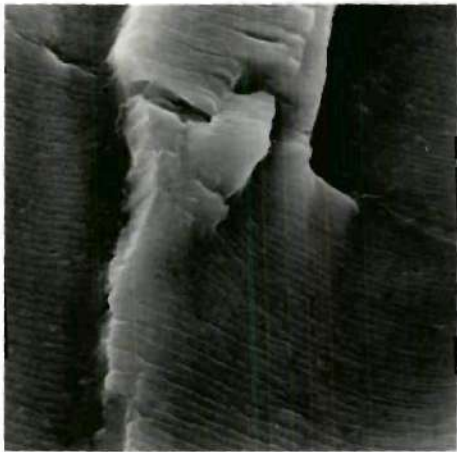
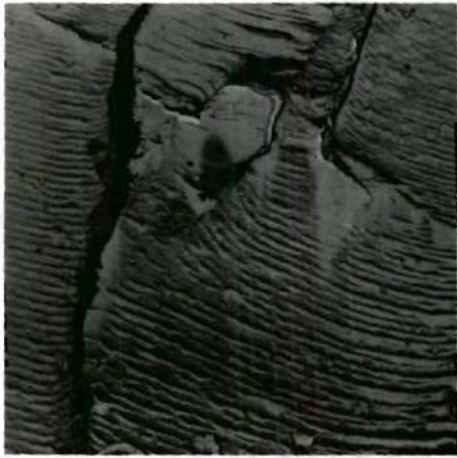


Figure 17. Comparison of TEM and SEM Fractography in Stress Corrosion of Al Alloy (on following page)

Material: Aluminum 7075

Heat Treatment: T6

Type of Test: Stress corrosion

Ultimate Strength: 85,000 psi typical

Test Environment: Exposed to water & hydrostatic pressures

Magnification of Fractographs: 1760X

Tilt of Single Scanning Micrograph: 30°

Appearance of Fracture: The fracture surface shows intergranular fracture, corrosion pits on grain faces, and some small areas of dimples.

Comparison Analysis: The transmission micrograph shows the intergranular nature of the fracture with peaks of replica indicating secondary cracking. The surface appears flat in general. The scanning micrograph emphasizes the intergranular fracture and secondary cracking. It is seen that the elevation of the left side is much lower than that of the right, indicating collapse in this area of the carbon replica.

The single tilted scanning micrograph shows the topography somewhat well without the use of stereo.

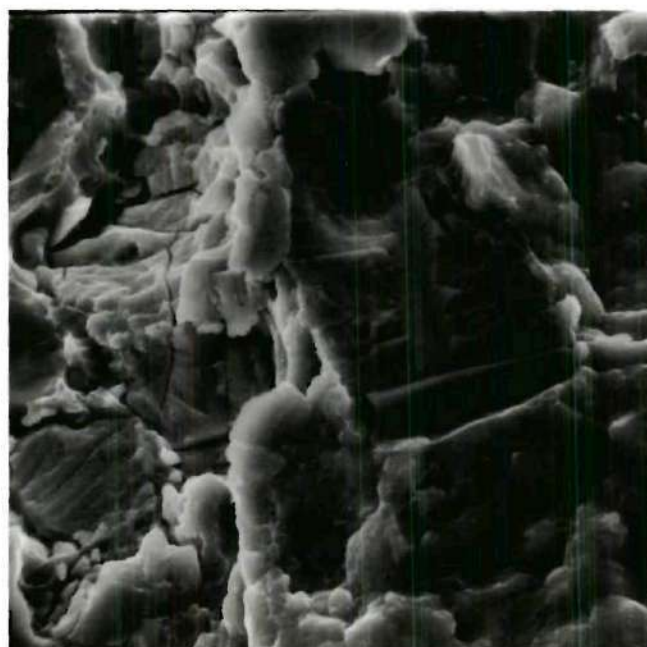
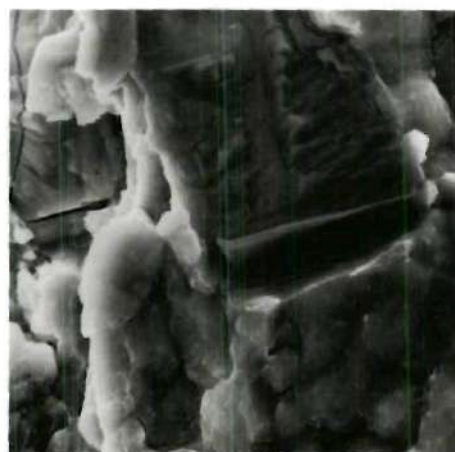
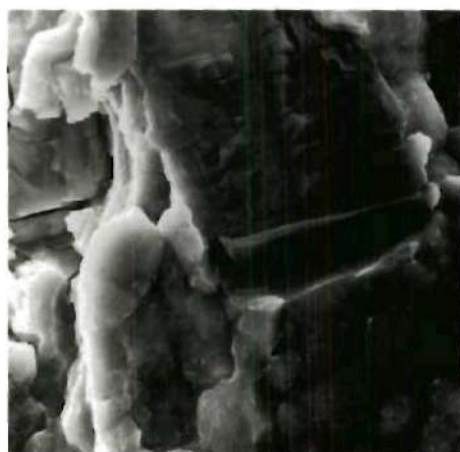


Figure 18. Comparison of TEM and SEM Fractography in Stress Corrosion of Al Alloy (on following page)

Material: Aluminum 7075

Heat Treatment: T6

Type of Test: Stress corrosion

Ultimate Strength: 85,000 psi typical

Test Environment: Exposed to water and hydrostatic pressures

Magnification of Fractographs: 3100X

Tilt of Single Scanning Micrograph: 30°

Appearance of Fracture: The fracture surface shows intergranular fracture, corrosion pits on grain faces, and some small areas of dimples.

Comparison Analysis: The transmission micrograph shows intergranular fracture, corrosion pits on grain faces, secondary cracking and the transgranular fracture of a secondary particle. The scanning micrograph reveals the nature of the surface much clearer except that the corrosion pits and grain facets are not resolved. The topographical match between the sample and replica is not perfect but quite good in most of the area of this picture.

The single tilted scanning micrograph shows the topography quite well without the use of stereo.

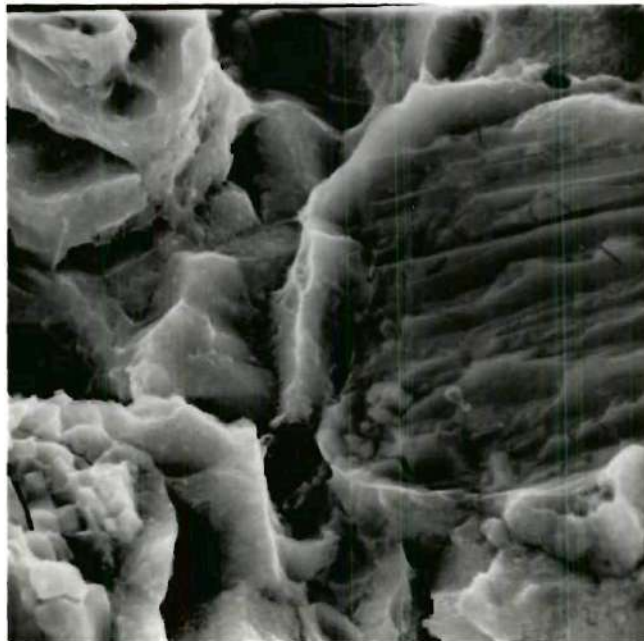
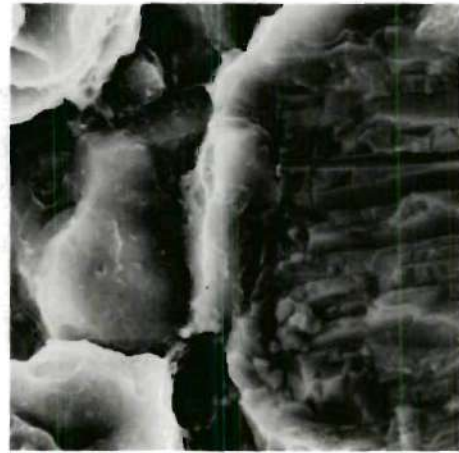
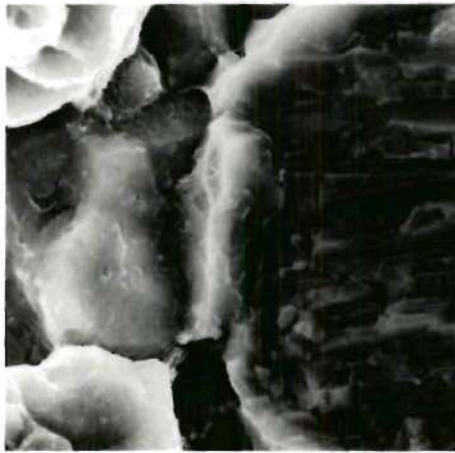


Figure 19. Comparison of TEM and SEM Fractography in Stress Corrosion of Al Alloy (on following page)

Material: Aluminum 7075

Heat Treatment: T6

Type of Test: Stress corrosion

Ultimate Strength: 85,000 psi typical

Test Environment: Exposed to water & hydrostatic pressures

Magnification of Fractographs: 4000X

Tilt of Single Scanning Micrograph: 30°

Appearance of Fracture: The fracture surface shows intergranular fracture, corrosion pits on exposed grain faces, and some small areas of dimples.

Comparison Analysis: The transmission micrograph reveals the intergranular nature of the fracture, peaks of replica film indicating secondary cracking, and an area of dimples. The scanning micrograph shows the intergranular nature and secondary cracking much more clearly. The elevation changes are seen to be much greater than indicated by the transmission micrograph indicating some collapse of the replica. The corrosion pits are not resolved in the scanning micrograph.

The single tilted scanning micrograph shows the topography well without the use of stereo.

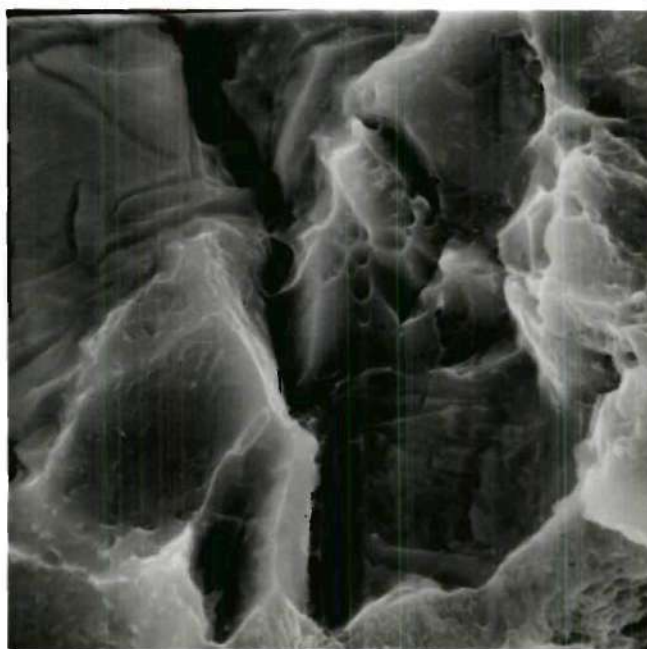
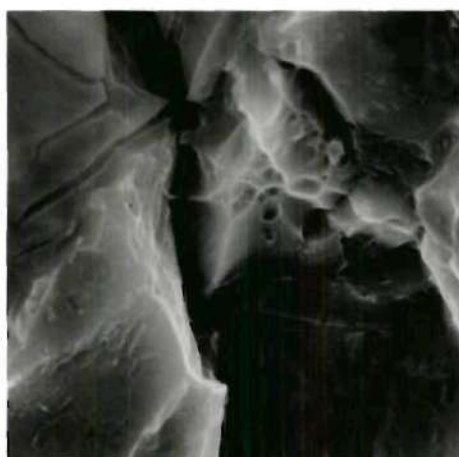
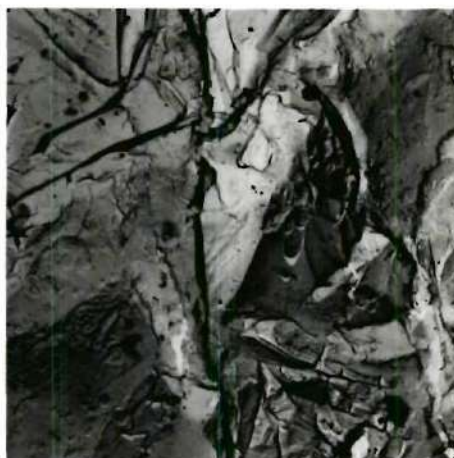


Figure 20. Comparison of TEM and SEM Fractography in Stress Corrosion of Al Alloy (on following page)

Material: Aluminum 7075

Heat Treatment: T6

Type of Test: Stress corrosion

Ultimate Strength: 85,000 psi typical

Test Environment: Exposed to water & hydrostatic pressures

Magnification of Fractographs: 5000X

Tilt of Single Scanning Micrograph: 30°

Appearance of Fracture: The fracture surface shows intergranular fracture, corrosion pits on exposed grain faces and some small areas of dimples.

Comparison Analysis: The transmission micrograph reveals the intergranular nature of the fracture and the corrosion on the grain surfaces. The peaks of replica causing dark areas around grains are due to replication of secondary cracks and grain separation. The scanning micrograph depicts much more clearly the intergranular fracture and the grain separation and secondary cracking. It does not show, however, the corrosion pits on the grain surfaces due to its lower resolution.

The single tilted scanning micrograph shows the topography well without the use of stereo.

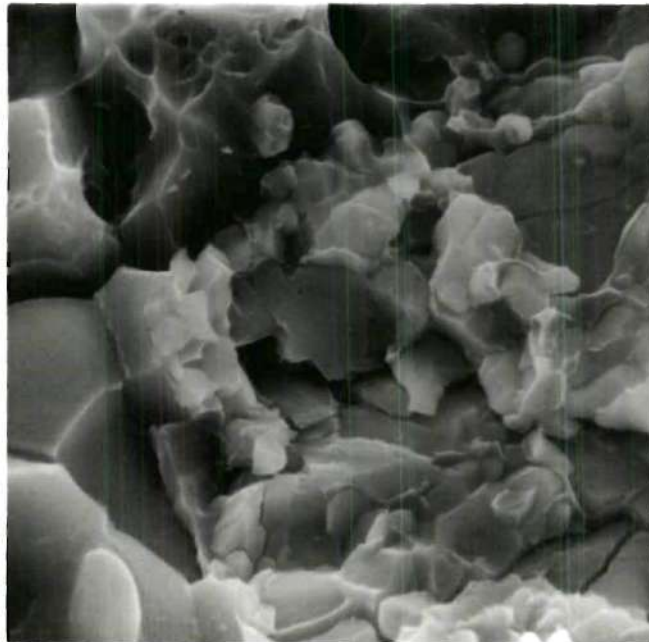
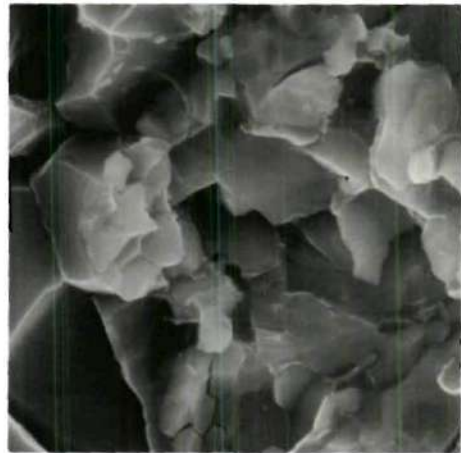
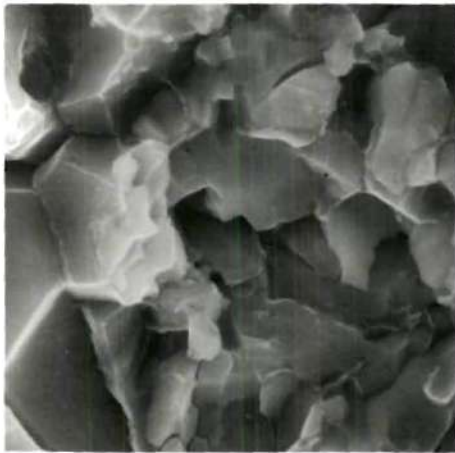
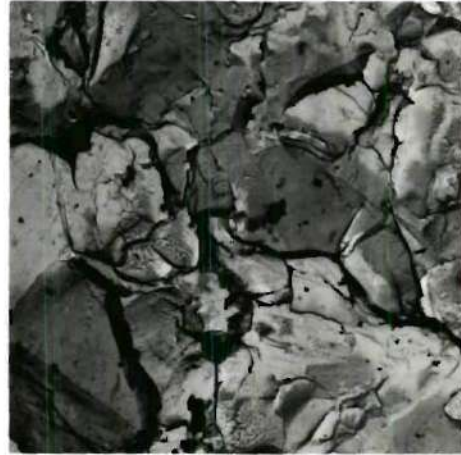
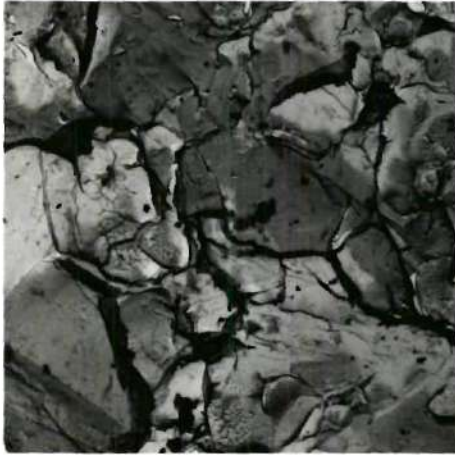


Figure 21. Comparison of TEM and SEM Fractography in Overload of 4340 Steel (on following page)

Material: Steel 4340

Heat Treatment: 1500°F, oil quench, tempered at 500°F

Type of Test: Overload; notched-tension

Ultimate Strength: 170,000 psi

Test Environment: Air at ambient temperature

Magnification of Fractographs: 3100X

Tilt of Single Scanning Micrograph: 40°

Appearance of Fracture: The fracture surface shows dimpled rupture with some secondary particles.

Comparison Analysis: The transmission micrograph shows the dimpled rupture. The dark feature at the top left appears to be torn and somewhat collapsed. The general area appears fairly flat. The scanning micrograph reveals that the dimples are actually on a steep incline running from bottom left to top right. The replication of the large deep dimple at top left resulted in the partially collapsed area of the transmission micrograph previously mentioned.

The single tilted scanning micrograph shows this area at an angle much nearer to the transmission presentation. The topography is not shown by this micrograph without the use of stereo.

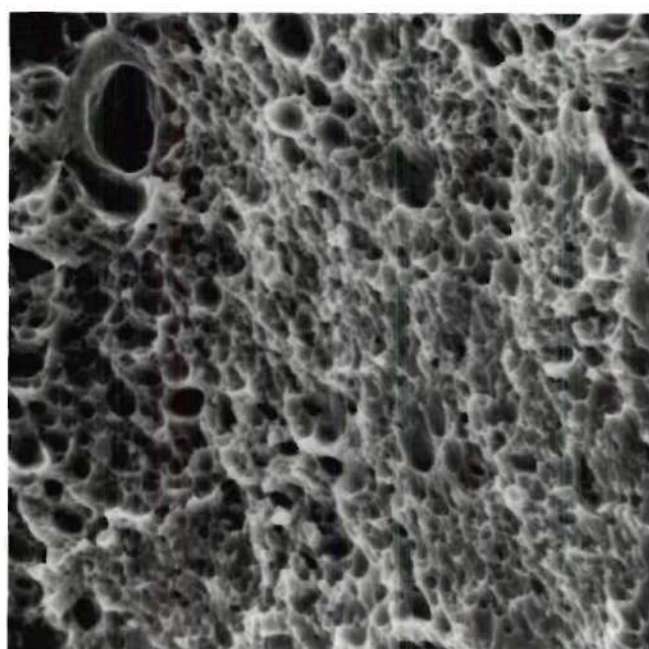
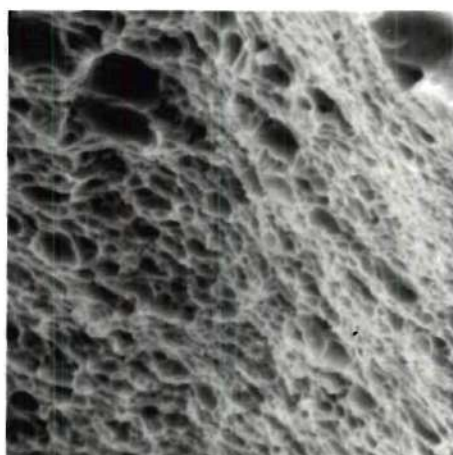
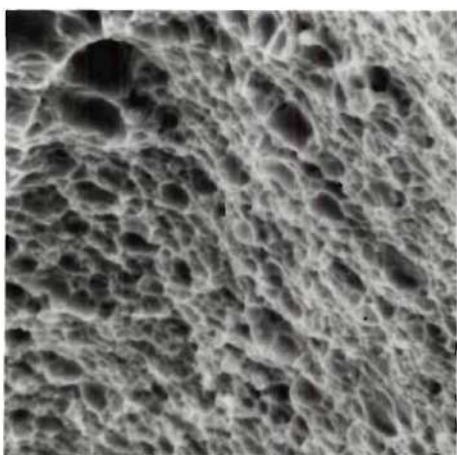


Figure 22. Comparison of TEM and SEM Fractography in Overload of 4340 Steel (on following page)

Material: Steel 4340

Heat Treatment: 1500°F, oil quench, tempered at 500°F

Type of Test: Overload; notched-tension

Ultimate Strength: 170,000 psi

Test Environment: Air at ambient temperature

Magnification of Fractographs: 4000X

Tilt of Single Scanning Micrograph: 30°

Appearance of Fracture: The fracture surface shows dimpled rupture with some secondary particles.

Comparison Analysis: The transmission micrograph shows the dimpled rupture. The general plane of these area appears fairly even. The scanning micrograph shows this area to have some quite different elevations. It demonstrates the fact that the replica has flattened out. Some of the features seen on the replica are features on the side of the wall which runs horizontally across the center of the scanning micrograph. The scanning micrograph also reveals secondary particles in some of the dimples.

The single tilted scanning micrograph reveals some of the side wall features seen on the transmission micrograph but hidden from view in the scanning stereo micrograph. The topography is shown to a small degree in this micrograph without the use of stereo.

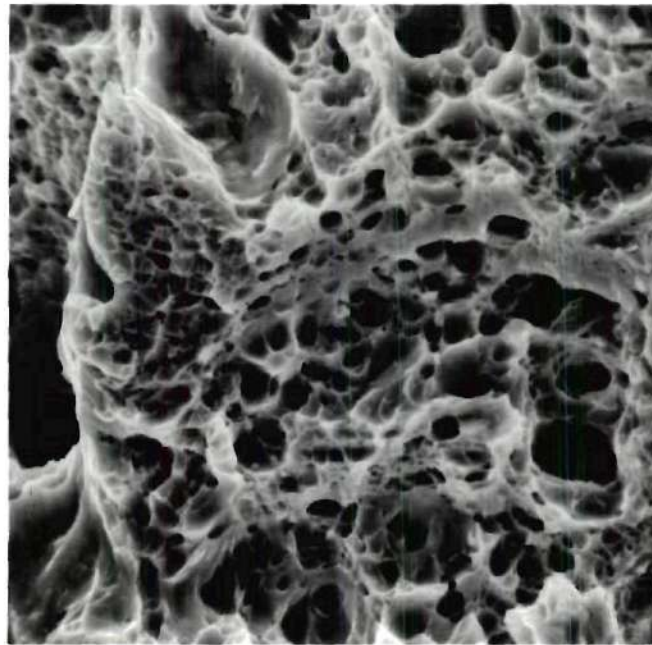
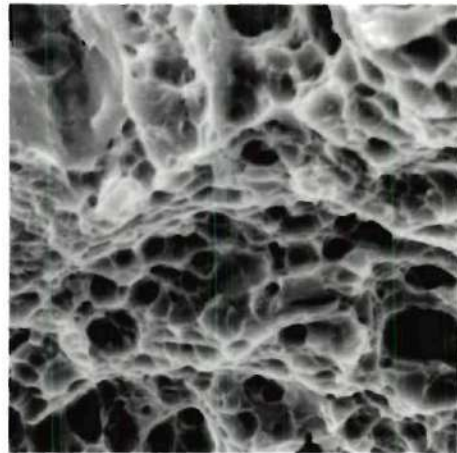
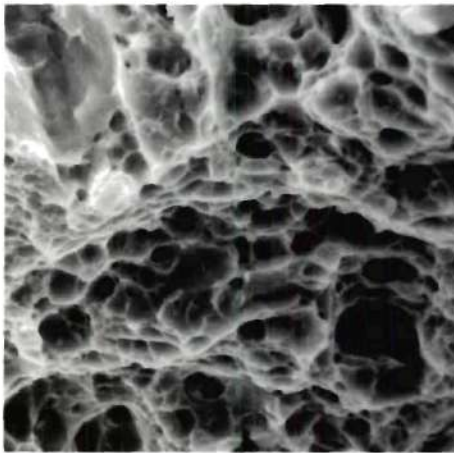


Figure 23. Comparison of TEM and SEM Fractography in Overload of 4340 Steel (on following page)

Material: Steel 4340

Heat Treatment: 1500°F, oil quench, tempered at 500°F

Type of Test: Overload; notched-tension

Ultimate Strength: 170,000 psi

Test Environment: Air at ambient temperature

Magnification of Fractographs: 6400X

Tilt of Single Scanning Micrograph: 40°

Appearance of Fracture: The fracture surface shows dimpled rupture with some secondary particles.

Comparison Analysis: The transmission micrograph shows the dimpled rupture. The circular feature at the bottom right is somewhat hard to interpret. The scanning micrograph reveals the true topography and the nature of the bottom right feature as a secondary particle in the large dimple. The topographical match between the replica and the surface is fair.

The single tilted scanning micrograph shows the topography quite well without the use of stereo.

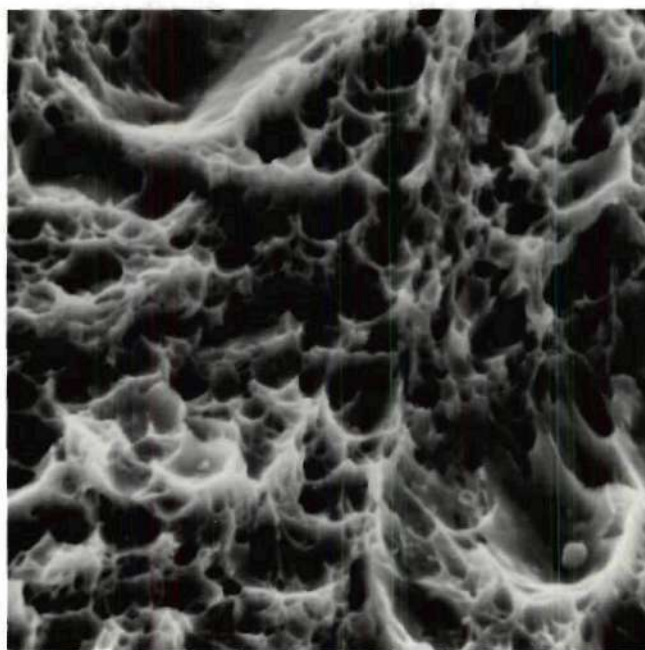
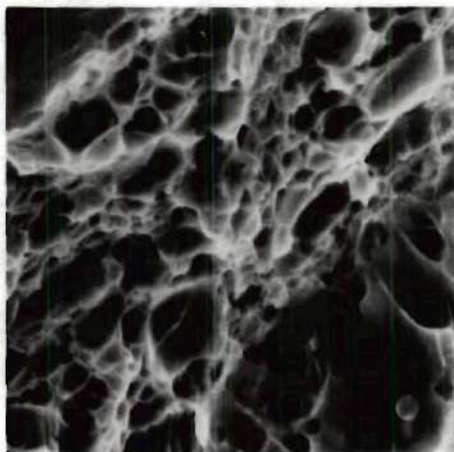
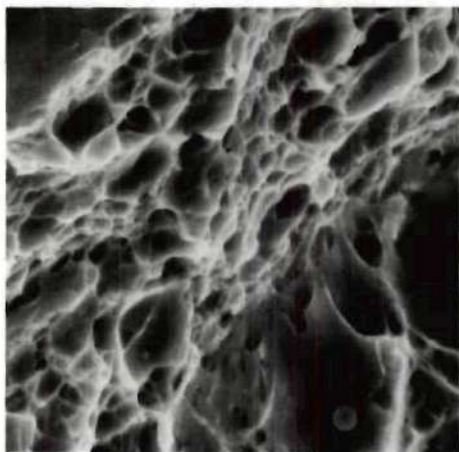


Figure 24. Comparison of TEM and SEM Fractography Fatigue of 4340 Steel (on following page)

Material: Steel 4340

Heat Treatment: 1500°F, oil quenched, tempered at 500°F

Type of Test: High cycle fatigue

Ultimate Strength: 170,000 psi typical

Test Environment: Air at ambient temperature

Magnification of Fractographs: 5250X

Tilt of Single Scanning Micrograph: 30°

Appearance of Fracture: The fracture surface is fairly flat with a rubbed appearance. The striations are not well defined.

Comparison Analysis: The transmission micrograph shows the faint fatigue striations. The topographical match between the replica and the sample surface as seen in the scanning micrograph is excellent in this area. The striations however are not resolved in the scanning micrograph.

The single tilted scanning micrograph shows the topography moderately well without the use of stereo. The orientation of this picture is turned 90° clockwise from that of the stereo pair.

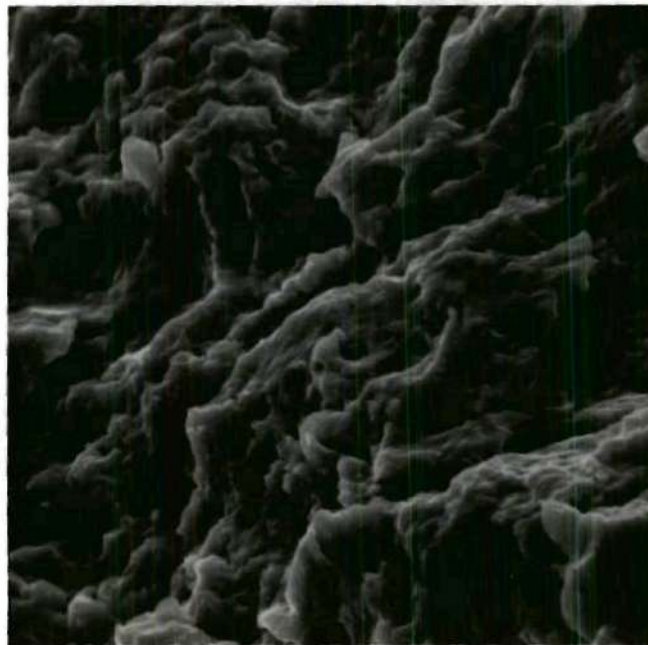
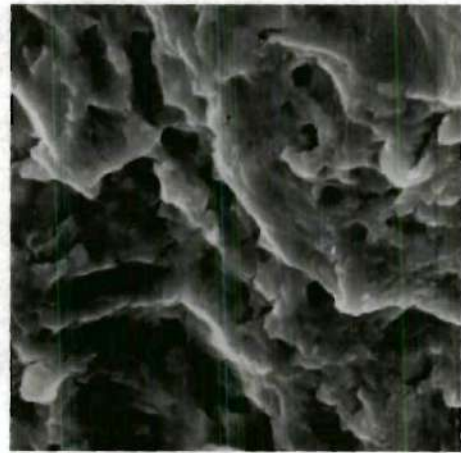
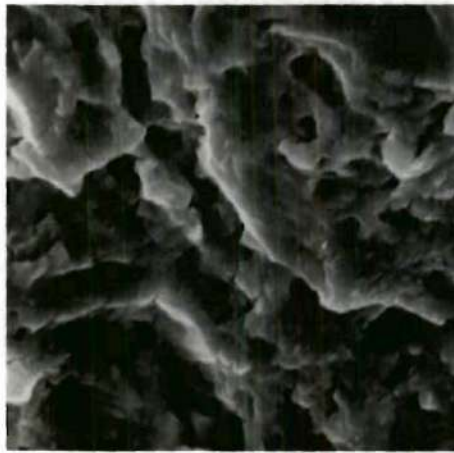


Figure 25. Comparison of TEM and SEM Fractography in Fatigue of 4340 Steel (on following page)

Material: Steel 4340

Heat Treatment: 1500°F, oil quenched, tempered at 500°F

Type of Test: High cycle fatigue

Ultimate Strength: 170,000 psi typical

Test Environment: Air at ambient temperature

Magnification of Fractographs: 10,080X

Tilt of Single Scanning Micrograph: 45°

Appearance of Fracture: The fracture surface is fairly flat and rubbed with poorly defined fatigue striations.

Comparison Analysis: It appears from the transmission micrograph that the surface is very flat with one small area in the center of striations. The scanning micrograph reveals that the surface is not flat at all. The fatigue striations are resolved although lack of contrast makes them less obvious.

The single tilted scanning micrograph show the topography very well without the use of stereo. The orientation of this picture is turned 90° clockwise from that of the stereo pair.

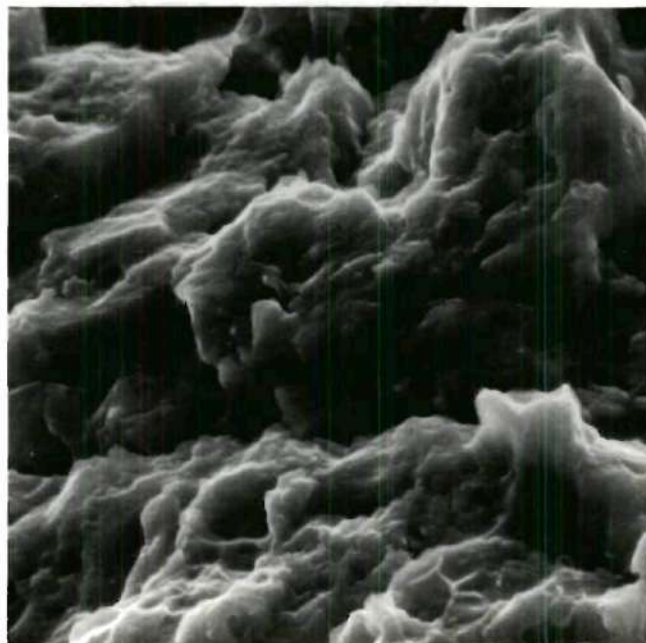
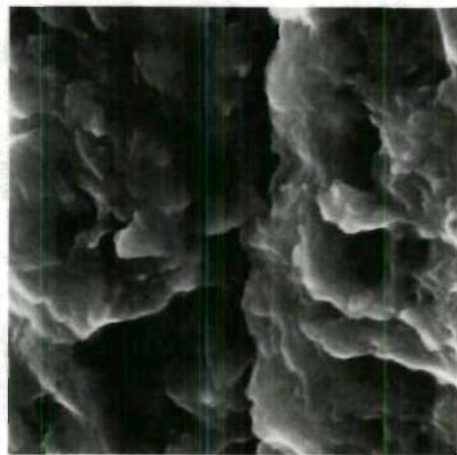
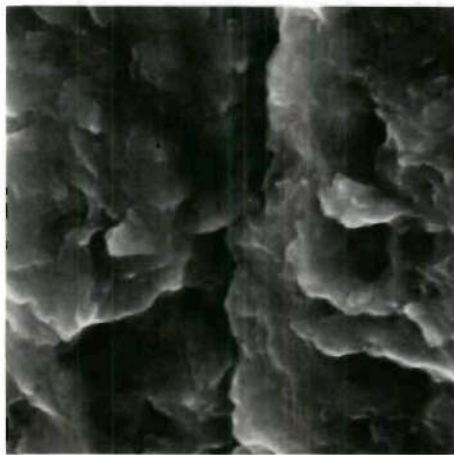
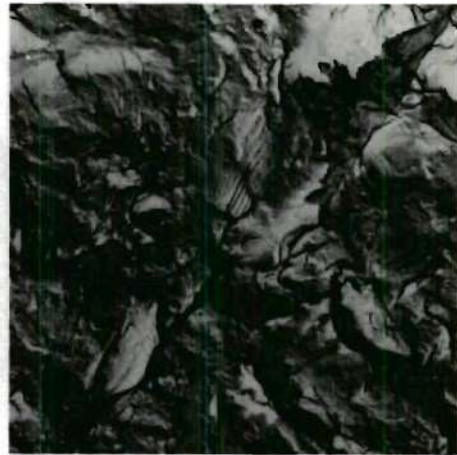


Figure 26. Comparison of TEM and SEM Fractography in Stress Corrosion of 4340 Steel (on following page)

Material: Steel 4340

Heat Treatment: 1500°F, oil quench, tempered at 500°F

Type of Test: Stress corrosion

Ultimate Strength: 170,000 psi typical

Test Environment: 3½% NaCl in water at ambient temperature

Magnification of Fractographs: 3200X

Tilt of Single Scanning Micrograph: 30°

Appearance of Fracture: The fracture surface is intergranular with secondary cracks and corrosion pits on grain faces.

Comparison Analysis: The transmission micrograph shows the intergranular nature of the fracture, the corrosion pits on grain faces, and wispy replica films coming up from grain boundary regions indicating secondary cracking. The scanning micrograph reveals the intergranular relief and secondary cracking with excellent detail but the corrosion pits are not resolved. Although the replica does not appear collapsed and shows proper depth, it is hard to match the features of the replica with those seen in the scanning micrograph. This is due to the slightly different angle at which the surface is presented in the two views.

The single tilted scanning micrograph shows the topography fairly well without the use of stereo. The orientation of this picture is turned 90° clockwise from that of the stereo.

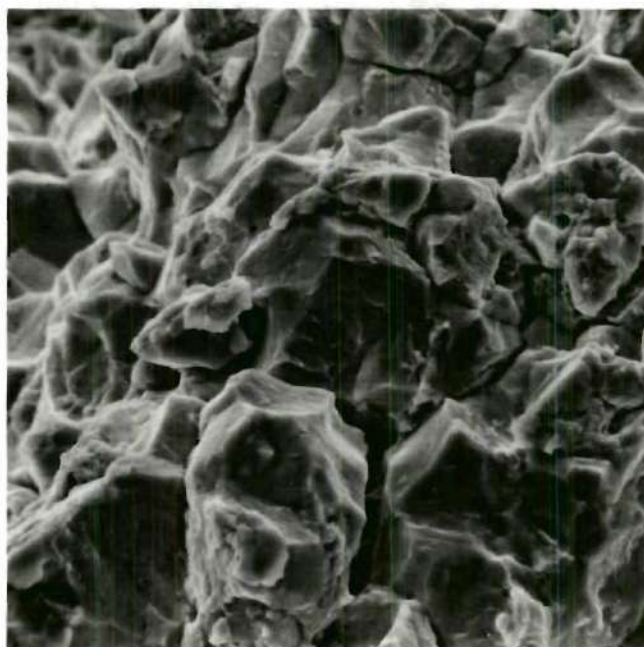
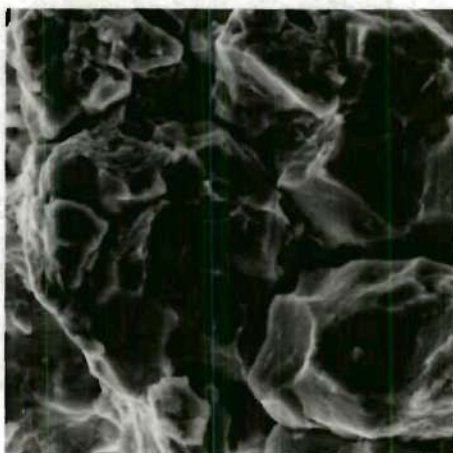
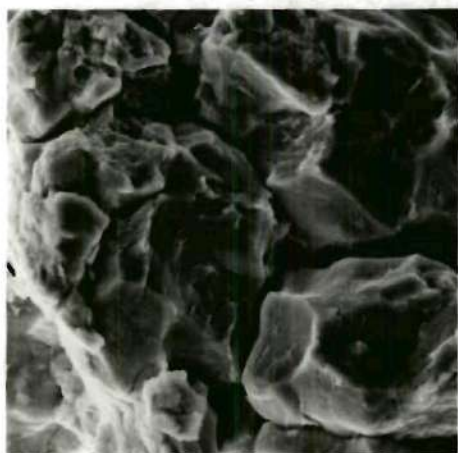


Figure 27. Comparison of TEM and SEM Fractography in Stress Corrosion of 4340 Steel (on following page)

Material: Steel 4340

Heat Treatment: 1500°F, oil quench, tempered at 500°F

Type of Test: Stress corrosion

Ultimate of Strength: 170,000 psi typical

Test Environment: 3½% NaCl in water at ambient temperature

Magnification of Fractographs: 10,080X

Tilt of Single Scanning Micrograph: 30°

Appearance of Fracture: The fracture surface is intergranular with secondary cracks and corrosion pits on grain faces.

Comparison Analysis: This high magnification transmission micrograph was taken to show the fine detail of the corrosion pits. The scanning micrograph does not resolve these pits. The transmission view is a bit rotated from the scanning view which makes matching of features somewhat difficult.

The single tilted scanning micrograph shows the topography to some extent without the use of stereo. The orientation of this picture is turned 90° clockwise from that of the stereo.

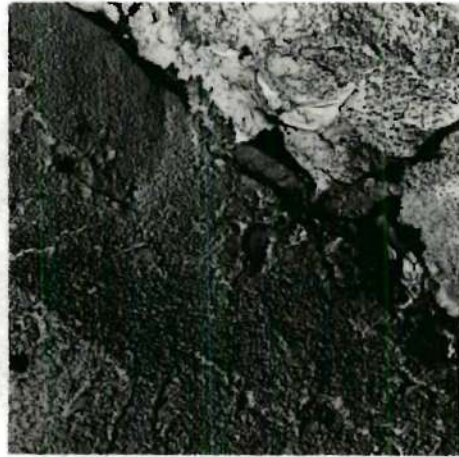
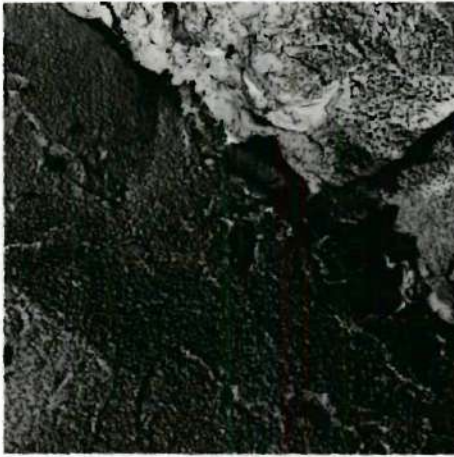


Figure 28. Comparison of TEM and SEM Fractography in Impact of High Speed Steel (on following page)

Material: High speed steel; 18W, 4Cr, 1C

Heat Treatment: 1200°C, oil quench, tempered at 500°C

Type of Test: Impact

Ultimate Strength: 400,000 psi (calculated from hardness)

Test Environment: Air at ambient temperature

Magnification of Fractographs: 2400X

Tilt of Single Scanning Micrograph: 30°

Appearance of Fracture: The fracture surface shows a mixture of intergranular separation and transgranular cleavage and quasi cleavage.

Comparison Analysis: The transmission micrograph shows mostly cleavage with some areas of intergranular separation. The river patterns on the cleavage faces are not well seen at this low magnification. The scanning micrograph reveals the true topography of this area well. Some of the river patterns on the cleavage faces can be seen but are not as clear or contrasty as in the transmission micrograph. The match between the surface and the replica are quite good.

The single tilted scanning micrograph shows the topography moderately well without the use of stereo.

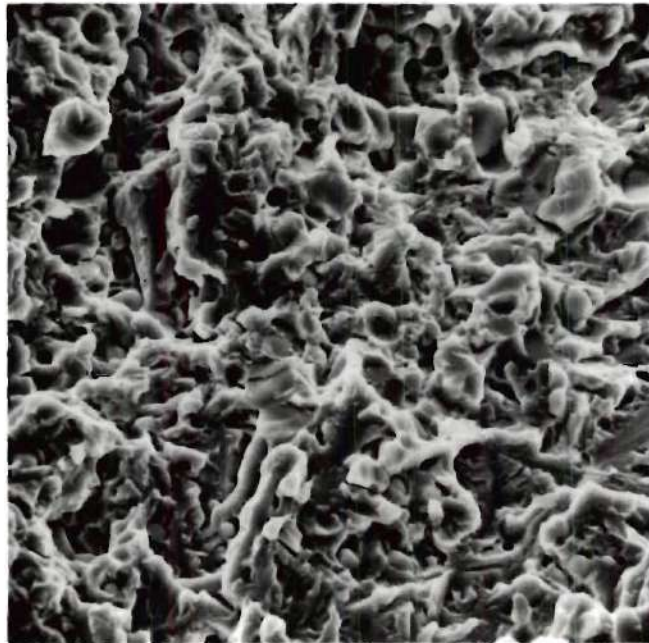
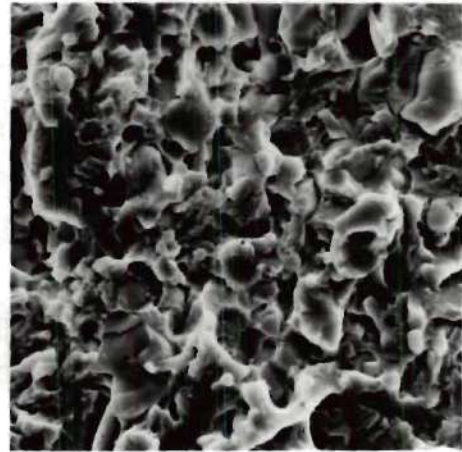
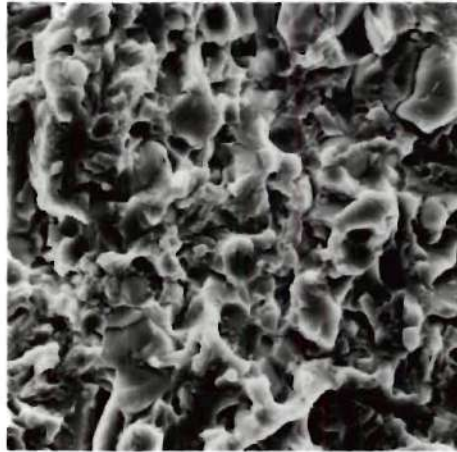


Figure 29. Comparison of TEM and SEM Fractography in Impact of High Speed Steel (on following page)

Material: High speed steel; 18W, 4Cr, 1C

Heat Treatment: 1200°C, oil quench, tempered at 500°C

Type of Test: Impact

Ultimate Strength: 400,000 psi (calculated from hardness)

Test Environment: Air at ambient temperature

Magnification of Fractographs: 3100X

Tilt of Single Scanning Micrograph: 30°

Appearance of Fracture: The fracture surface shows a mixture of intergranular separation and transgranular cleavage and quasi cleavage.

Comparison Analysis: The transmission micrograph reveals cleavage and intergranular separation. River patterns are easily seen on the cleavage faces. The scanning micrograph shows the true topography of this area very well. The river patterns can be seen but are not as clear or contrasty as they are in the transmission micrograph. The match between the surface and the replica is very good even though the bottoms of some deep holes are not completely replicated.

The single tilted scanning micrograph shows the topography moderately well without the use of stereo.

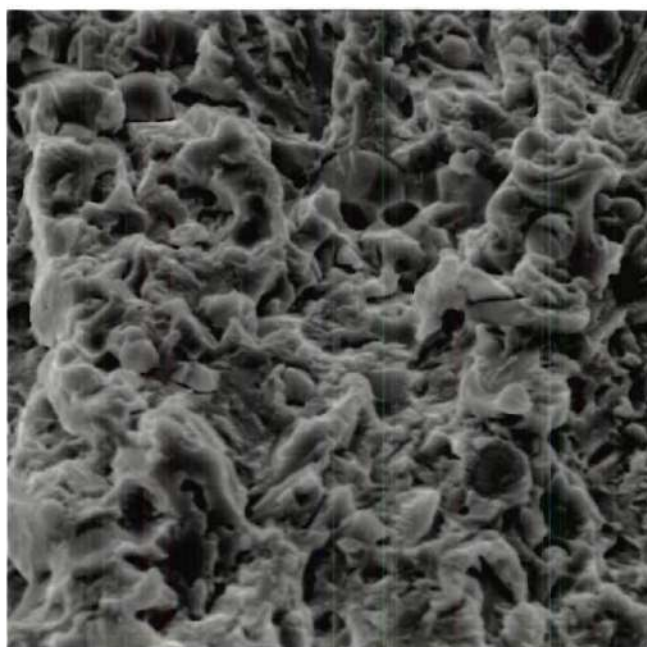
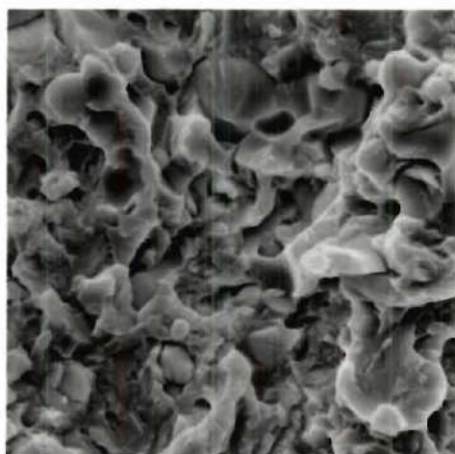
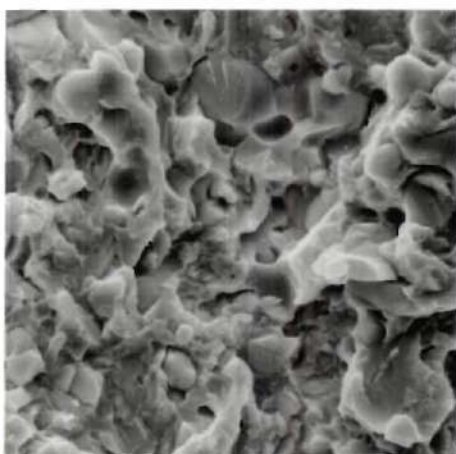


Figure 30. Comparison of TEM and SEM Fractography Impact of High Speed Steel (on following page)

Material: High speed steel, 18W, 4Cr, 1C

Heat Treatment: 1200°C, oil quench, tempered at 500°C

Type of Test: Impact

Ultimate Strength: 400,000 psi (calculated from hardness)

Test Environment: Air at ambient temperature

Magnification of Fractographs: 4000X

Tilt of Single Scanning Micrograph: 30°

Appearance of Fracture: The fracture surface shows a mixture of intergranular separation and transgranular cleavage and quasi cleavage.

Comparison Analysis: The transmission micrograph shows cleavage and intergranular separation. The river patterns on cleavage faces are easily seen. The scanning micrograph reveals the true topography of this area very well. River patterns are not as well seen, however, the match between the surface and the replica is very good.

The single tilted scanning micrograph shows the topography moderately well without the use of stereo.

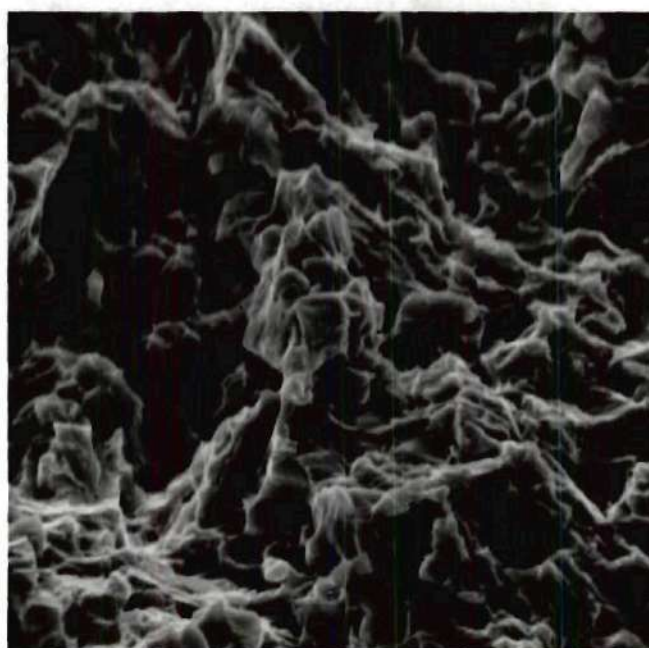
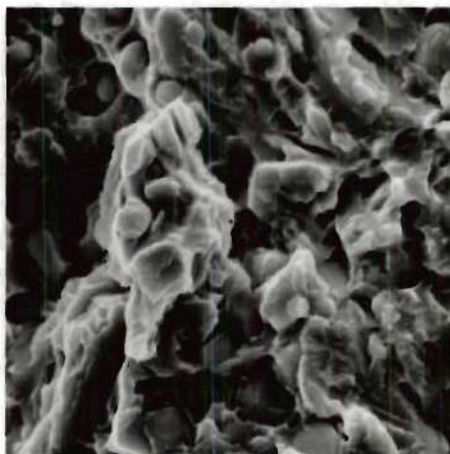
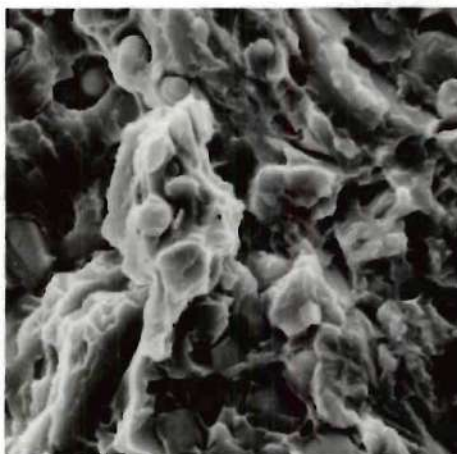


Figure 31. Comparison of TEM and SEM Fractography in Impact of Plain Carbon Steel (on following page)

Material: Plain carbon steel

Heat Treatment: Oil quenched, tempered at 150°C

Type of Test: Impact

Ultimate Strength: 400,000 psi (calculated from hardness)

Test Environment: Air at ambient temperature

Magnification of Fractographs: 2400X

Tilt of Single Scanning Micrograph: 30°

Appearance of Fracture: The fracture surface shows a mixture of dimples, intergranular separation, and transgranular cleavage and quasi cleavage.

Comparison Analysis: The transmission micrograph shows dimples and intergranular separation with a few areas of transgranular cleavage. The thin peaks of replica indicate some deep holes or cracks in the surface. The scanning micrograph reveals the true topography of these area and demonstrates the nature of the holes and cracks very well.

The single tilted scanning micrograph does not show the topography too well, without the use of stereo.

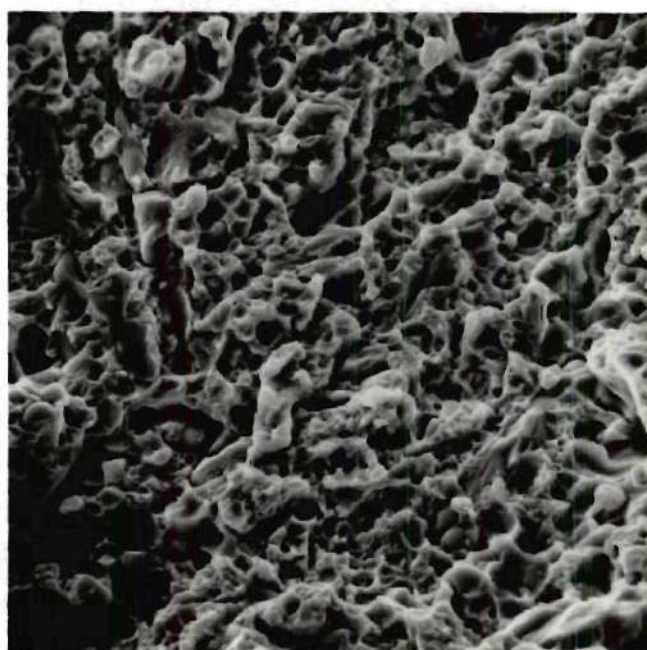
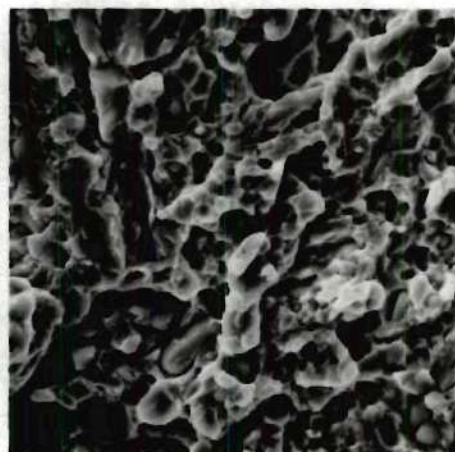
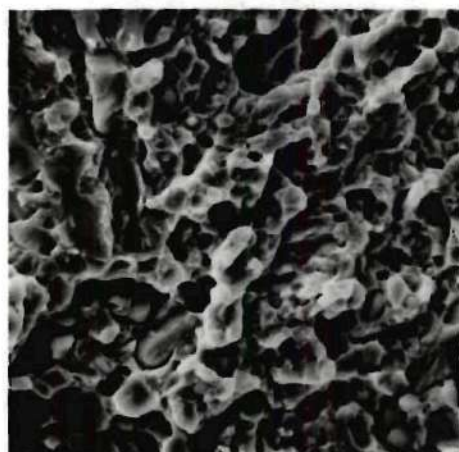
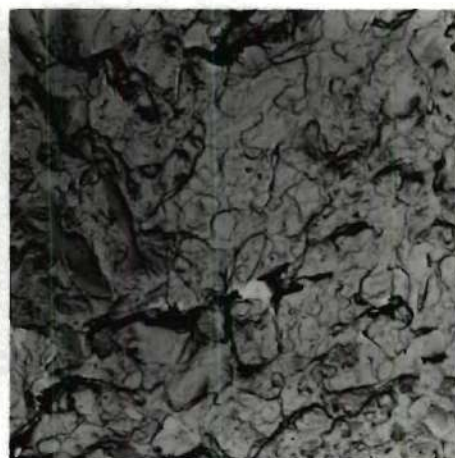


Figure 32. Comparison of TEM and SEM Fractography in Impact of Plain Carbon Steel (on following page)

Material: Plain carbon steel

Heat Treatment: Oil quench, tempered at 150°C

Type of Test: Impact

Ultimate Strength: 400,000 psi (calculated from hardness)

Test Environment: Air at ambient temperature

Magnification of Fractographs: 3100X

Tilt of Single Scanning Micrograph: 30°

Appearance of Fracture: The fracture surface shows a mixture of dimples, intergranular separation, and transgranular cleavage and quasi cleavage.

Comparison Analysis: The transmission micrograph shows an area of quasi cleavage in the center with other areas of cleavage, dimples and intergranular separation. The overlapped replica film appears a bit crumpled and may indicate collapse or simply irregular crevices. The scanning micrograph reveals that this area has more elevational changes than shown in the transmission micrograph, indicating some collapse of the replica. The detail of the topography is excellent but the river patterns on cleavage face are not well resolved.

The single tilted scanning micrograph shows the topography moderately well without the use of stereo.

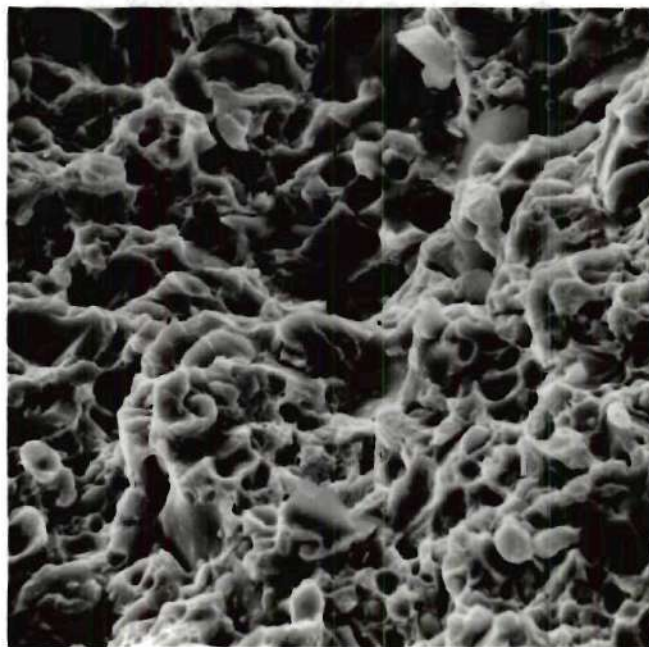
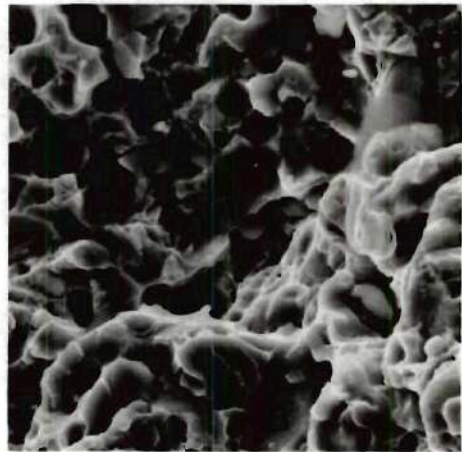
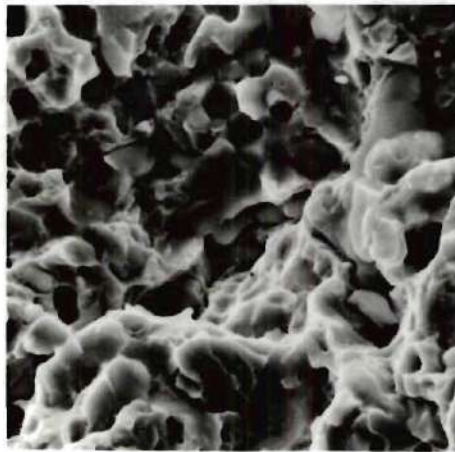
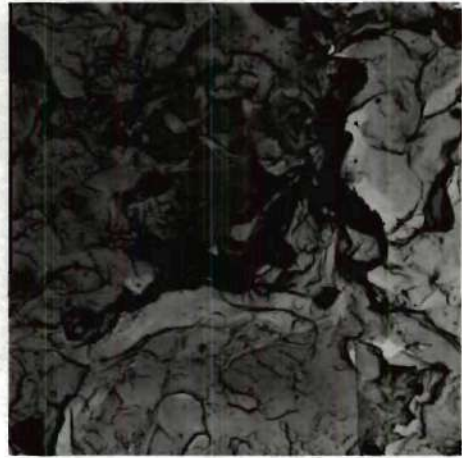
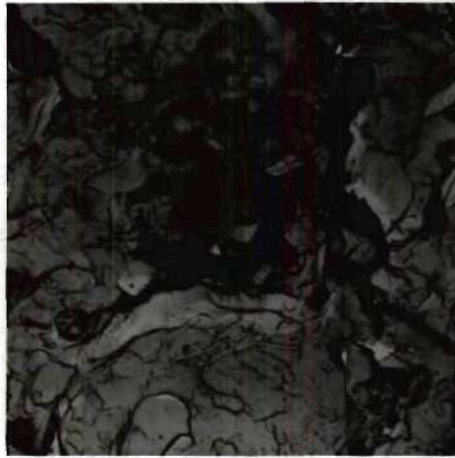


Figure 33. Comparison of TEM and SEM Fractography in Impact of Plain Carbon Steel (on following page)

Material: Plain carbon steel

Heat Treatment: Oil quench, tempered at 150°C

Type of Test: Impact

Ultimate Strength: 400,000 psi (calculated from hardness)

Test Environment: Air at ambient temperature

Magnification of Fractographs: 4000X

Tilt of Single Scanning Micrograph: 30°

Appearance of Fracture: The fracture surface shows a mixture of dimples, intergranular separation, and transgranular cleavage and quasi cleavage.

Comparison Analysis: The transmission micrograph shows intergranular separation, dimples, and cleavage. River patterns are well defined. There appears to be some collapse of the replica near the center of the micrograph. The scanning micrograph shows the topography to be much more irregular than shown in the transmission micrograph proving the suspected collapse of the replica. Some deep river patterns are seen but all are not resolved.

The single tilted scanning micrograph shows the topography fairly well without the use of stereo.

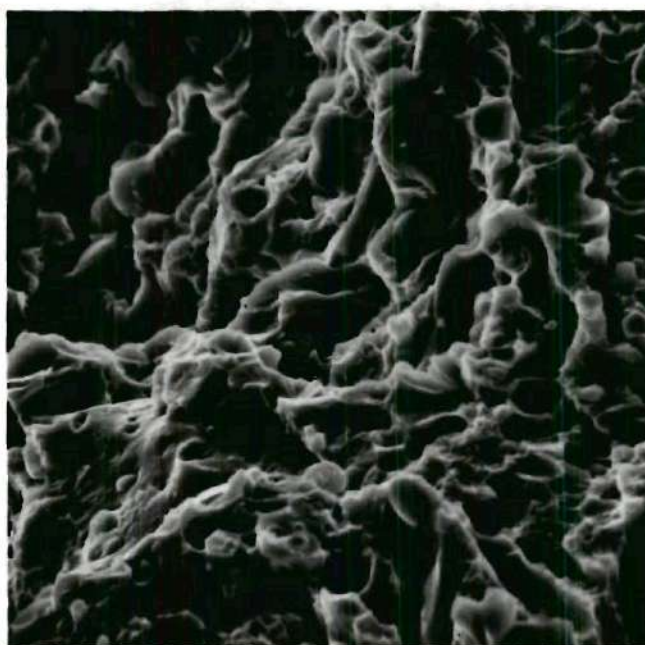
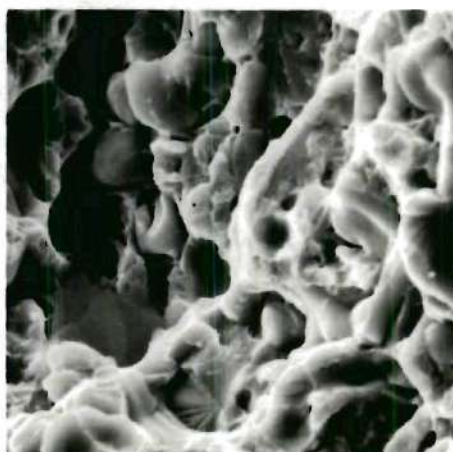
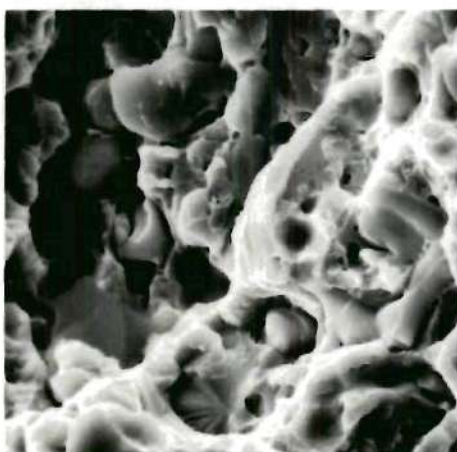
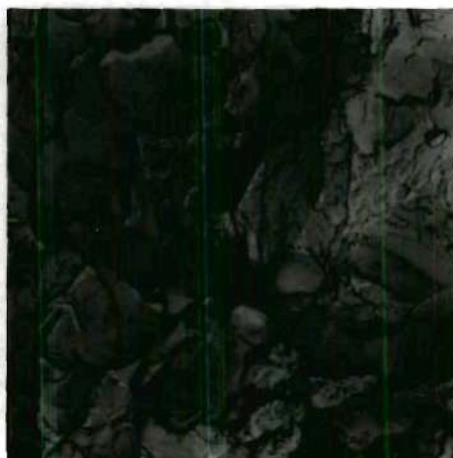
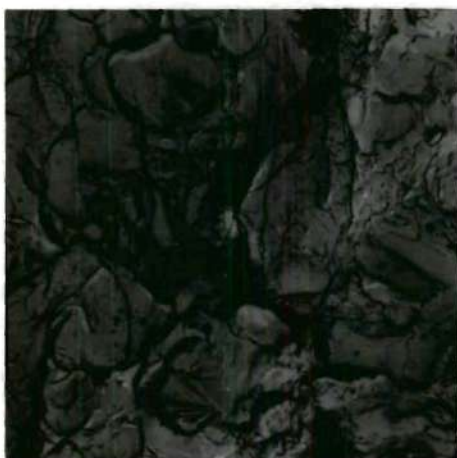


Figure 34. Comparison of TEM and SEM Fractography in Impact of Low Alloy Mn Steel (on following page)

Material: Steel; .6-.7C, 1-1.2Mn

Heat Treatment: Oil quenched

Type of Test: Impact

Ultimate Strength: Unknown

Test Environment: Air at ambient temperature

Magnification of Fractographs: 3100X

Tilt of Single Scanning Micrograph: 30°

Appearance of Fracture: The fracture surface shows mostly dimple rupture with second phase particles and areas of cleavage and stretch.

Comparison Analysis: The transmission micrograph shows an area of shear dimples. The scanning micrograph reveals these dimples to be normal tension type but on a sloping wall. This entire area of the replica has apparently fallen over. Second phase particles are seen in some of the dimples.

The single tilted scanning micrograph shows this area in much the same perspective as the transmission micrograph. The topography is not shown too well without the use of stereo.

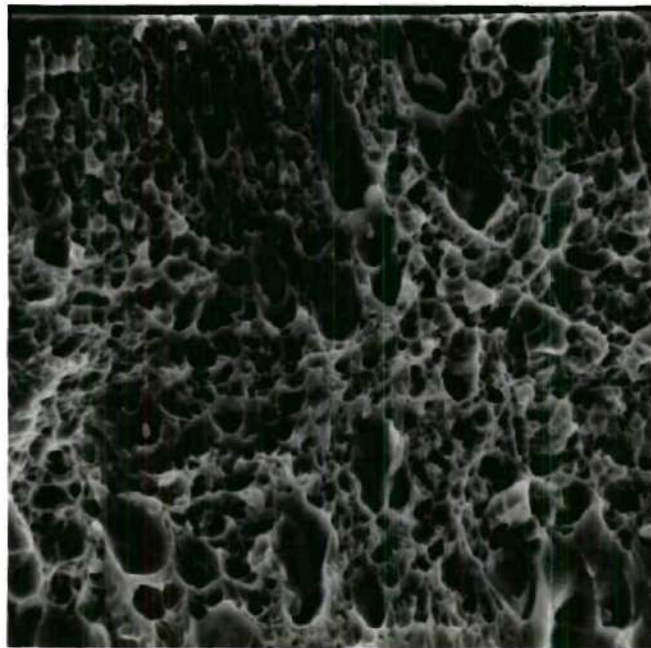
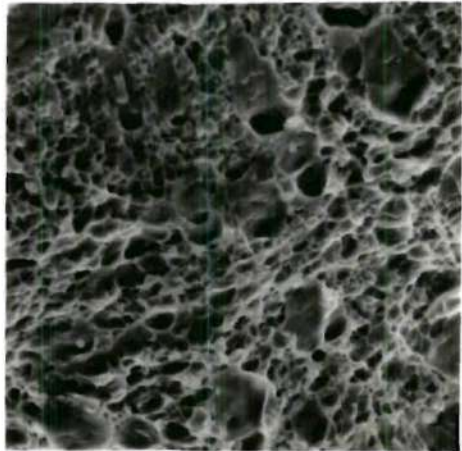
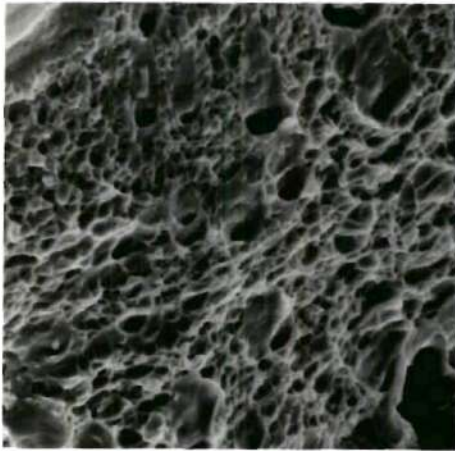


Figure 35. Comparison of TEM and SEM Fractography in Impact of Low Alloy Mn Steel (on following page)

Material: Steel; .6-.7C, 1-1.2Mn

Heat Treatment: Oil quenched

Type of Test: Impact

Ultimate Strength: Unknown

Test Environment: Air at ambient temperature

Magnification of Fractographs: 4000X

Tilt of Single Scanning Micrograph: 30°

Appearance of Fracture: The fracture surface shows mostly dimple rupture with second phase particles and areas of cleavage and stretch.

Comparison Analysis: The transmission micrograph shows some dimples and large smooth areas of stretching. The peaks of replica represent deep holes or dimples. The overlapped film on the left appears to be due to replica collapse. The scanning micrograph reveals the true topography and reveals the small secondary particles at the bottom of some of the dimples. The deep hole on the left confirms replica collapse of this area.

The single tilted scanning micrograph does not show the topography too well without the use of stereo.

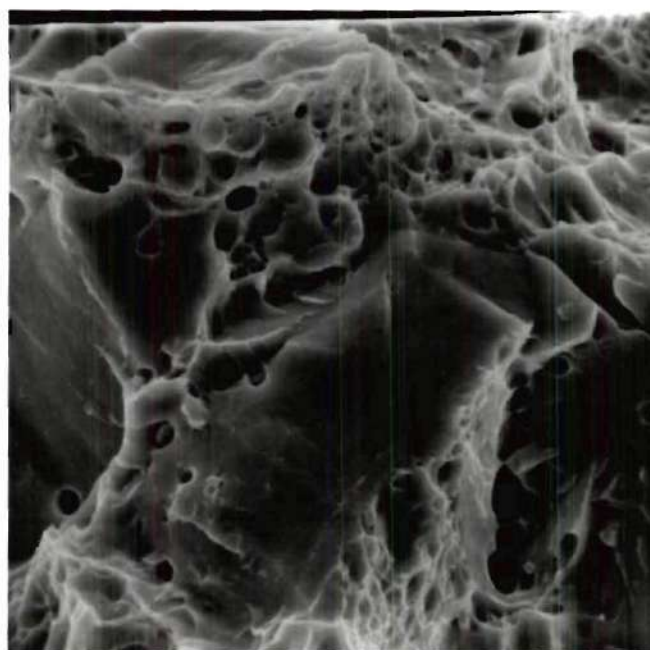
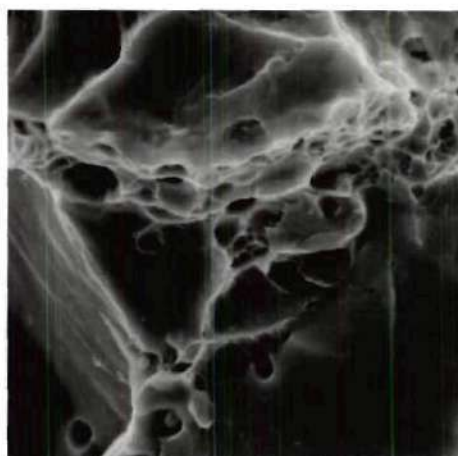
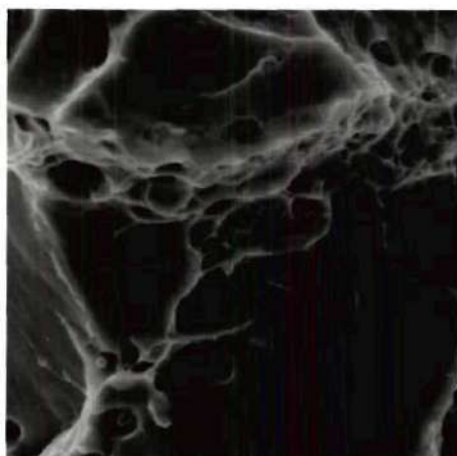


Figure 36. Comparison of TEM and SEM Fractography in Overload of Ti 8-1-1 Alloy (on following page)

Material: Titanium; 8Al, 1Mo, 1V

Heat Treatment: Annealed

Type of Test: Overload; notched-tension

Ultimate Strength: 145,000 psi

Test Environment: Air at ambient temperature

Magnification of Fractographs: 2400X

Tilt of Single Scanning Micrograph: 30°

Appearance of Fracture: The fracture surface consists mostly of fairly large dimples with some stretched areas and second phase particles.

Comparison Analysis: The transmission micrograph shows the coarse dimples typical of this fracture type. There are some areas of stretching. There is some folding of the replica and some peaks of replica due to incomplete replication of deep pits. The scanning micrograph reveals the true topography of this area with excellent clarity. It also reveals the existence of cubic phase particles mostly at the bottom of dimples which are not shown well in the transmission micrograph.

The single tilted scanning micrograph shows the topography well without the use of stereo.

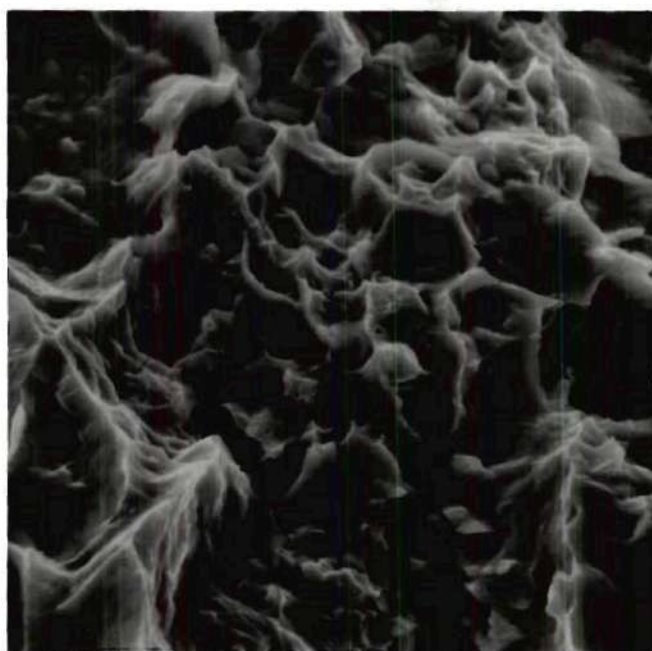
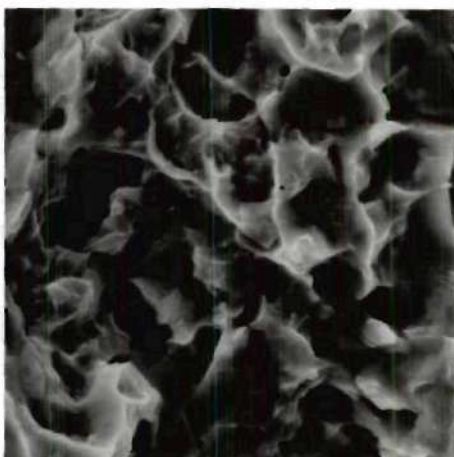
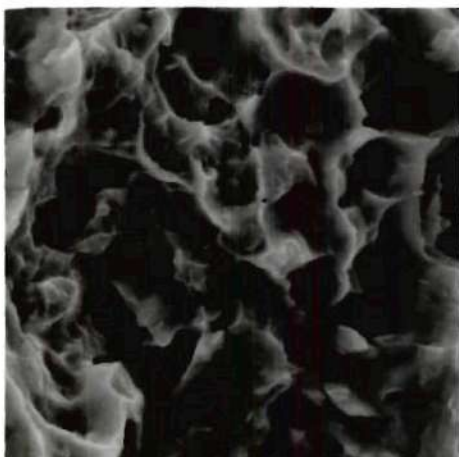


Figure 37. Comparison of TEM and SEM Fractography in Overload of Ti 8-1-1 Alloy (on following page)

Material: Titanium; 8Al, 1Mo 1V

Heat Treatment: Annealed

Type of Test: Overload; notched tension

Ultimate Strength: 145,000 psi

Test Environment: Air at ambient temperature

Magnification of Fractographs: 4000X

Tilt of Single Scanning Micrograph: 30°

Appearance of Fracture: The fracture surface consists mostly of fairly large dimples with some stretched areas and second phase particles.

Comparison Analysis: The transmission micrograph shows the large dimples and a stretched area. Some of the cubic phase particles can also be seen but they are somewhat hard to distinguish as such. The scanning micrograph reveals the proper topography very well. The stretch marks are well resolved and the cubic phase particles are easily distinguished.

The single tilted scanning micrograph shows the topography well without the use of stereo.

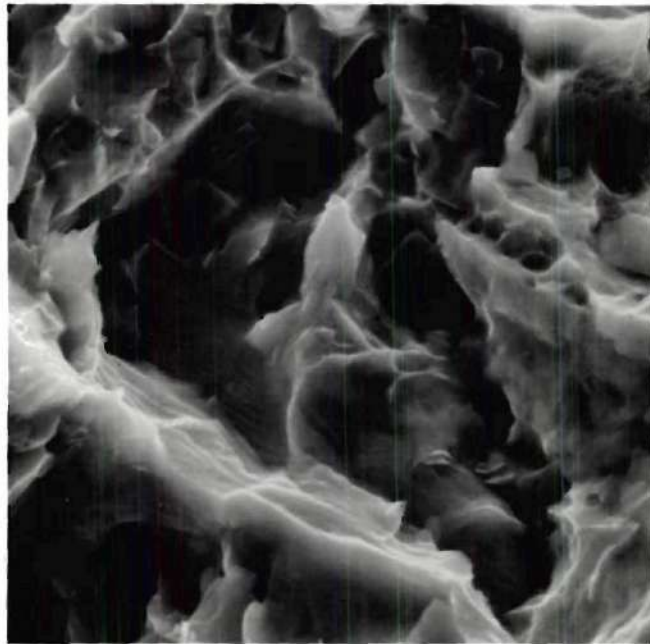
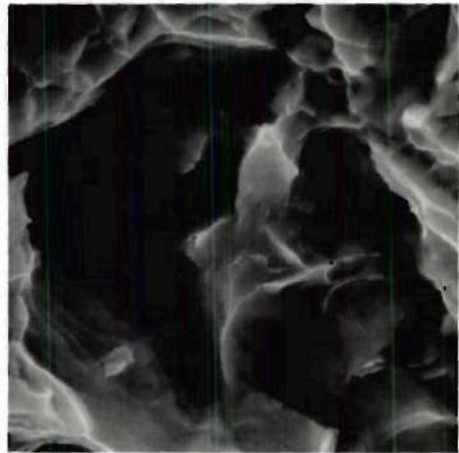
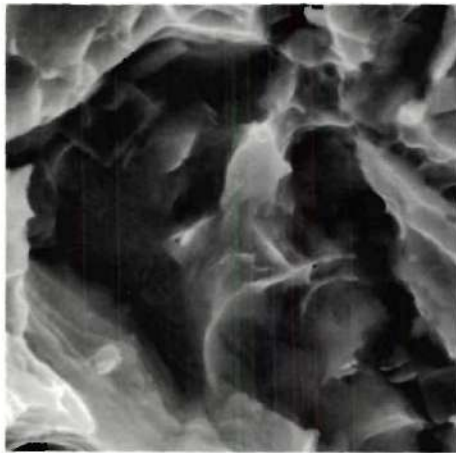


Figure 38. Comparison of TEM and SEM Fractography in Overload of Ti 8-1-1 Alloy (on following page)

Material: Titanium; 8Al, 1Mo, 1V

Heat Treatment: Annealed

Type of Test: Overload; notched-tension

Ultimate Strength: 145,000 psi

Test Environment: Air at ambient temperature

Magnification of Fractographs: 4000X

Tilt of Single Scanning Micrograph: 30°

Appearance of Fracture: The fracture surface consists mostly of large dimples with some stretched areas and second phase particles.

Comparison Analysis: The transmission micrograph shows the large dimples and some stretched areas. The feature in the center left which appears in the replica to be a depressed area with a fairly smooth surface is an artifact caused by an entrapped air bubble in the plastic replica medium. The scanning micrograph reveals the true topography very well. The stretch marks are resolved and the true nature of the area hidden by the artifact in the transmission micrograph is revealed.

The single tilted scanning micrograph shows the topography somewhat well without the use of stereo.

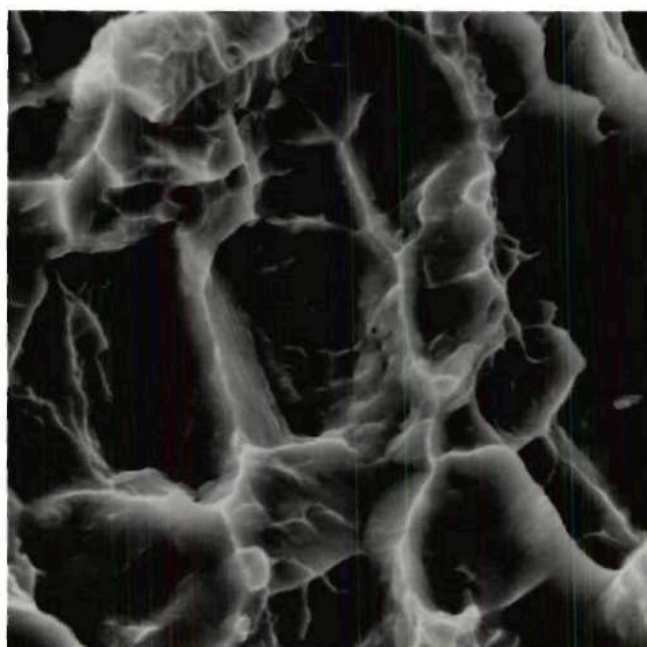
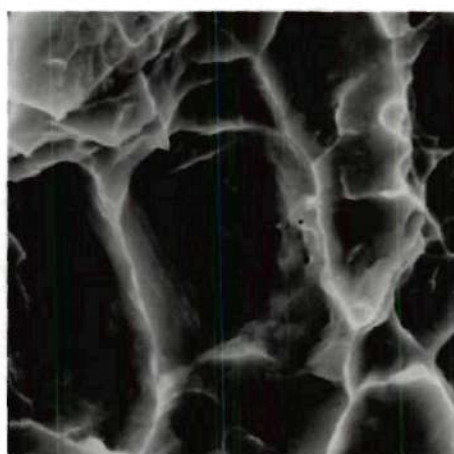
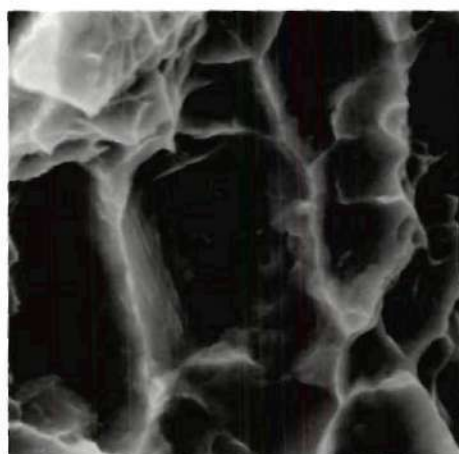


Figure 39. Comparison of TEM and SEM Fractography in Fatigue of Ti 3-1-1 Alloy (on following page)

Material: Titanium; 8Al, 1Mo, 1V

Heat Treatment: Annealed

Type of Test: High cycle fatigue

Ultimate Strength: 145,000 psi typical

Test Environment: Air at ambient temperature

Magnification of Fractographs: 1200X

Tilt of Single Scanning Micrograph: 30°

Appearance of Fracture: The fracture surface consists mostly of well defined widely spaced fatigue striations.

Comparison Analysis: The transmission micrograph shows the fatigue striations very well. This entire area appears fairly flat and there are some torn and overlapped features on the replica. The scanning micrograph reveals the true topography of the striations very nicely. The right hand feature rises from the striated surface quite sharply. The replica of these feature has apparently fallen over.

The single tilted scanning micrograph does not show the topography too well without the use of stereo.

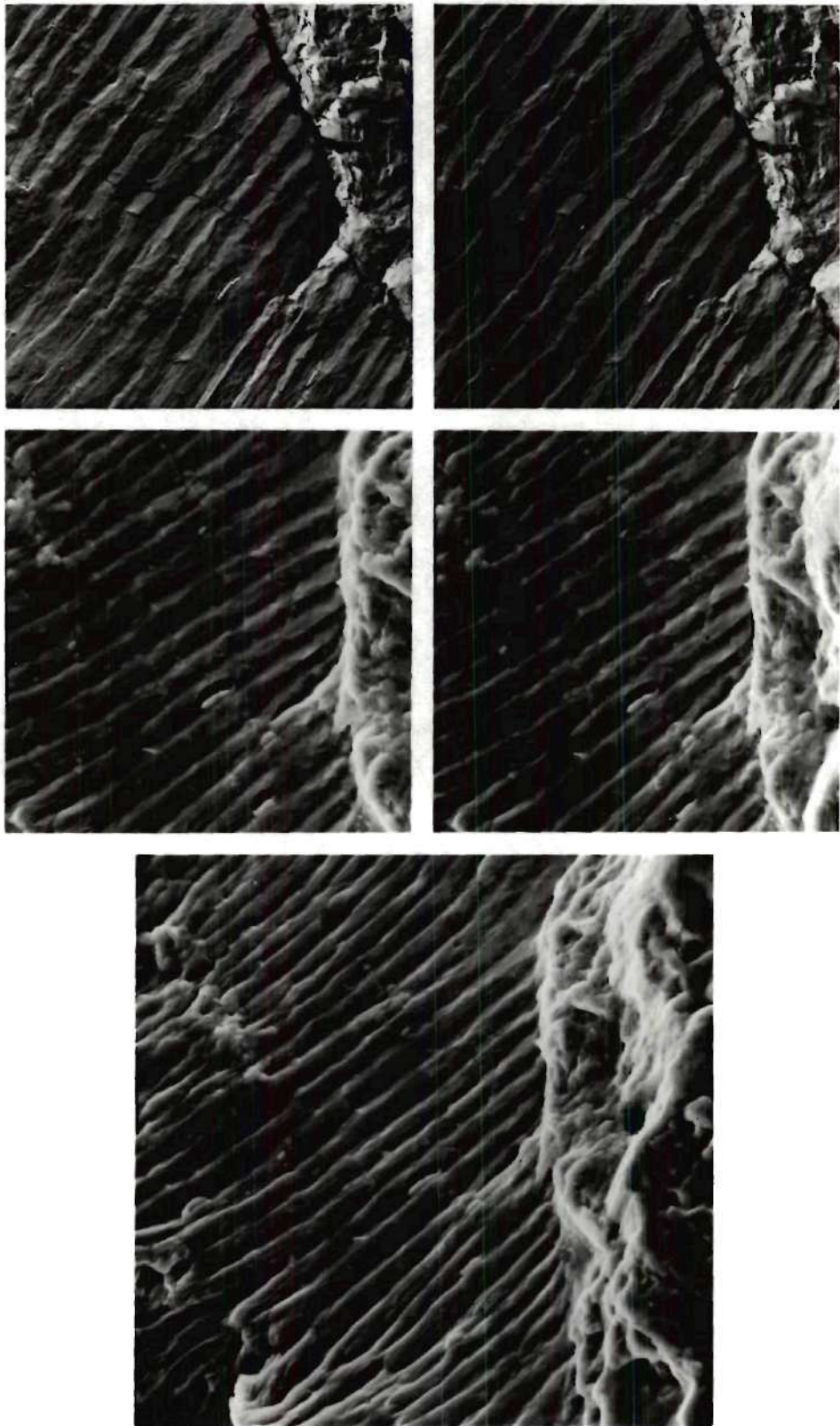


Figure 40. Comparison of TEM and SEM Fractography in Fatigue of Ti 8-1-1 Alloy (on following page)

Material: Titanium; 8Al, 1Mo, 1V

Heat Treatment: Annealed

Type of Test: High Cycle Fatigue

Ultimate Strength: 145,000 psi typical

Test Environment: Air at ambient temperature

Magnification of Fractographs: 2400X

Tilt of Single Scanning Micrograph: 30°

Appearance of Fracture: The fracture surface consists mostly of well defined widely spaced fatigue striations.

Comparison Analysis: The transmission micrograph reveals the large fatigue striations well. Stretch lines can be seen on the sides of the striations. The scanning micrograph shows the true topography of the striations very nicely. The stretch lines are not as well defined as in the transmission micrograph but can be seen. The match between the topographical features of the two micrographs is excellent.

The single tilted scanning micrograph does not show the topography too well without the use of stereo.

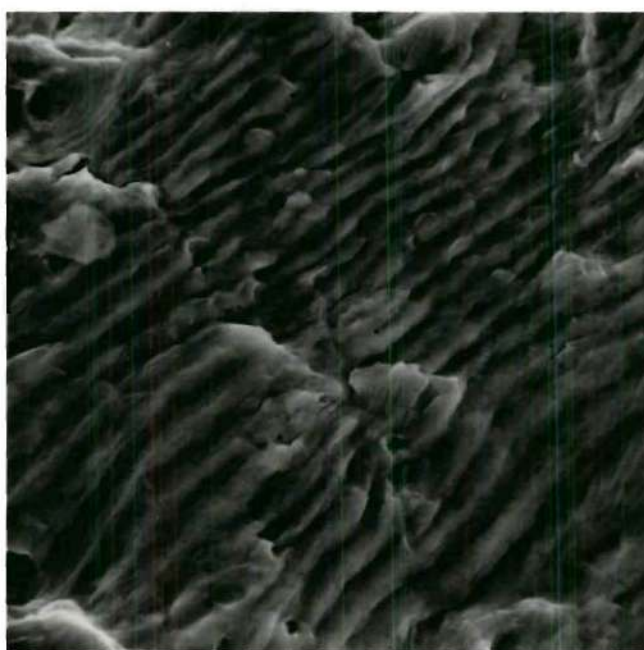
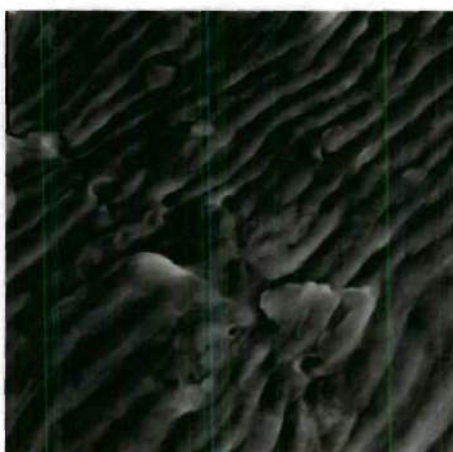
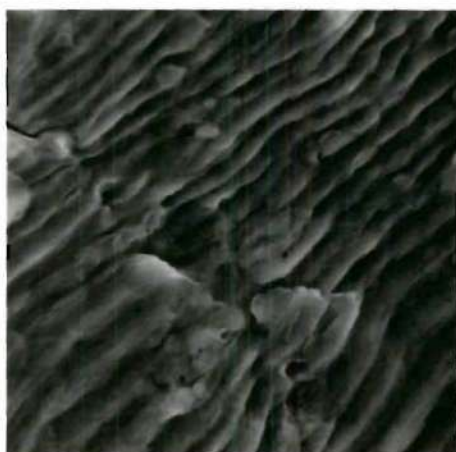
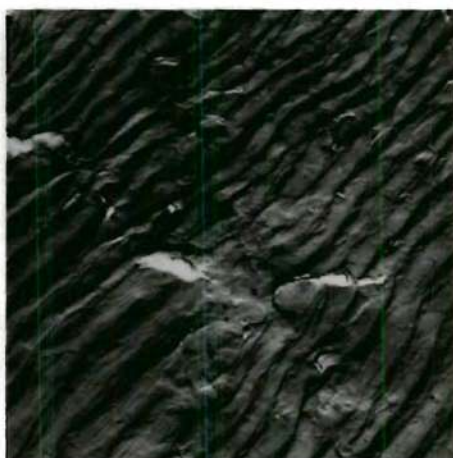
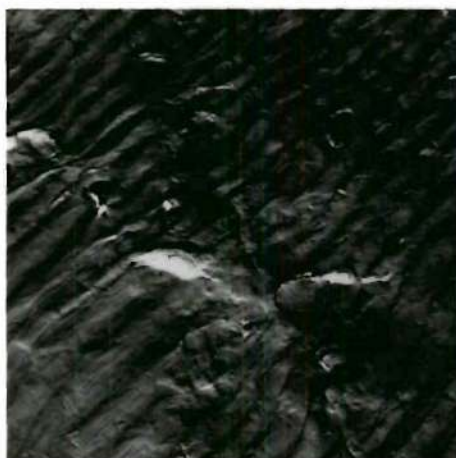


Figure 41. Comparison of TEM and SEM Fractography in Fatigue of Ti 8-1-1 Alloy (cn following page)

Material: Titanium; 8Al, 1Mo, 1V

Heat Treatment: Annealed

Type of Test: High cycle fatigue

Ultimate Strength: 145,000 psi typical

Test Environment: Air at ambient temperature

Magnification of Fractographs: 3100X

Tilt of Single Scanning Micrograph: 30°

Appearance of Fracture: The fracture surface consists mostly of well defined widely spaced fatigue striations.

Comparison Analysis: The transmission micrograph shows the striations and the juncture of two planes of striations very well. Stretch marks are well resolved. The scanning micrograph reveals the true topography of this area nicely. The stretch marks are not as contrasty but are well resolved. The match between this area of the surface and its replica is excellent.

The single tilted scanning micrograph shows the topography to some degree without the use of stereo.

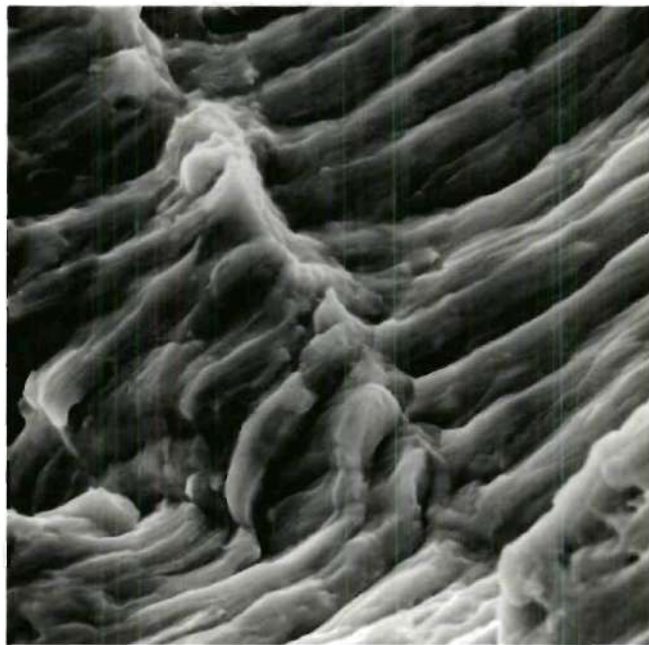
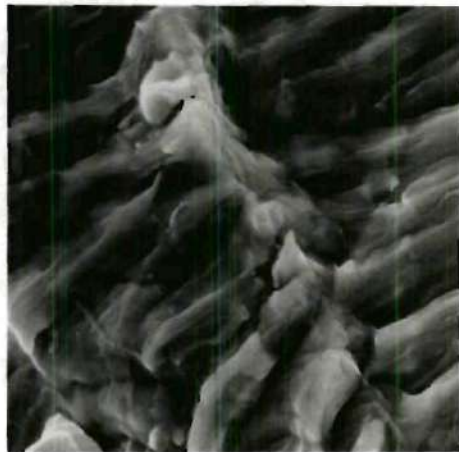
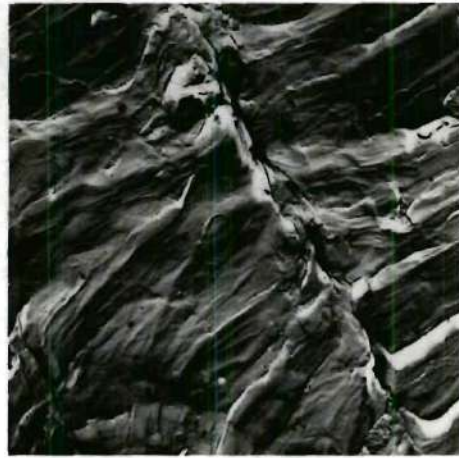


Figure 42. Comparison of TEM and SEM Fractography in Stress Corrosion of Ti 8-1-1 Alloy (on following page)

Material: Titanium; 8Al, 1Mo, 1V

Heat Treatment: Annealed

Type of Test: Stress corrosion

Ultimate Strength: 145,000 psi typical

Test Environment: 3½% NaCl in water at ambient temperature

Magnification of Fractographs: 3100X

Tilt of Single Scanning Micrograph: 30°

Appearance of Fracture: The fracture surface shows non-classic cleavage typical of stress corrosion cracking in this alloy.

Comparison Analysis: The transmission micrograph shows the cleavage surfaces nicely. The torn and overlapped areas indicate possible collapse of the replica. The scanning micrograph shows that this area is sloped considerably and demonstrates that the replica has not only collapsed some within this area but that this whole area of the replica has fallen over.

The single tilted scanning micrograph does not show the topography too well without the use of stereo.

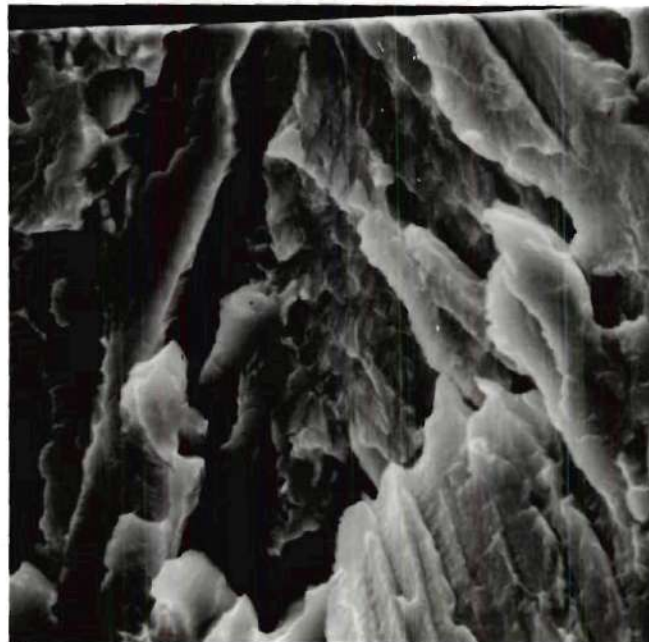
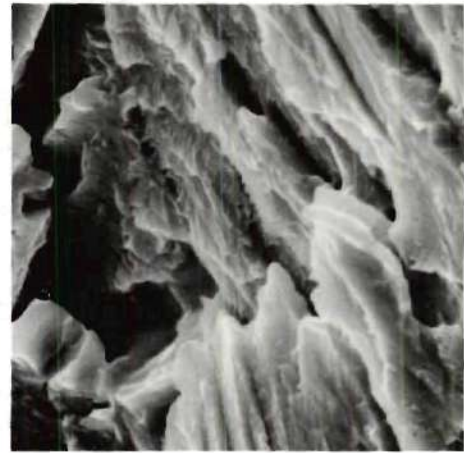
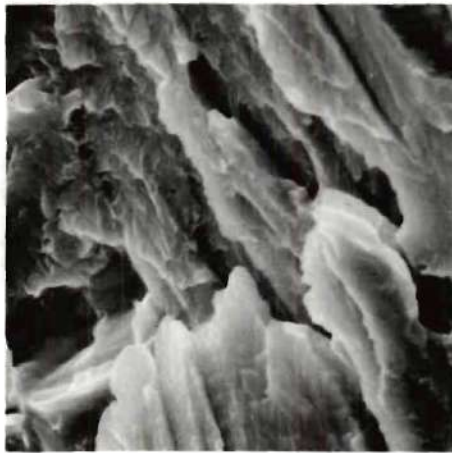


Figure 43. Comparison of TEM and SEM Fractography in Stress Corrosion of Ti 8-1-1 Alloy (on following page)

Material: Titanium; 8Al, 1Mo, 1V

Heat Treatment: Annealed

Type of Test: Stress corrosion

Ultimate Strength: 145,000 psi typical

Test Environment: 3½% NaCl in water at ambient temperature

Magnification of Fractographs: 3100X

Tilt of Single Scanning Micrograph: 30°

Appearance of Fracture: The fracture surface shows non-classic cleavage typical of stress corrosion cracking in this alloy.

Comparison Analysis: The transmission micrograph shows the cleavage surfaces well. The feature at the top left is an artifact caused by an entrapped bubble in the plastic replica medium. The scanning micrograph reveals the true topography although some of the fine surface details are not resolved.

The single tilted scanning micrograph shows the topography moderately well without the use of stereo.

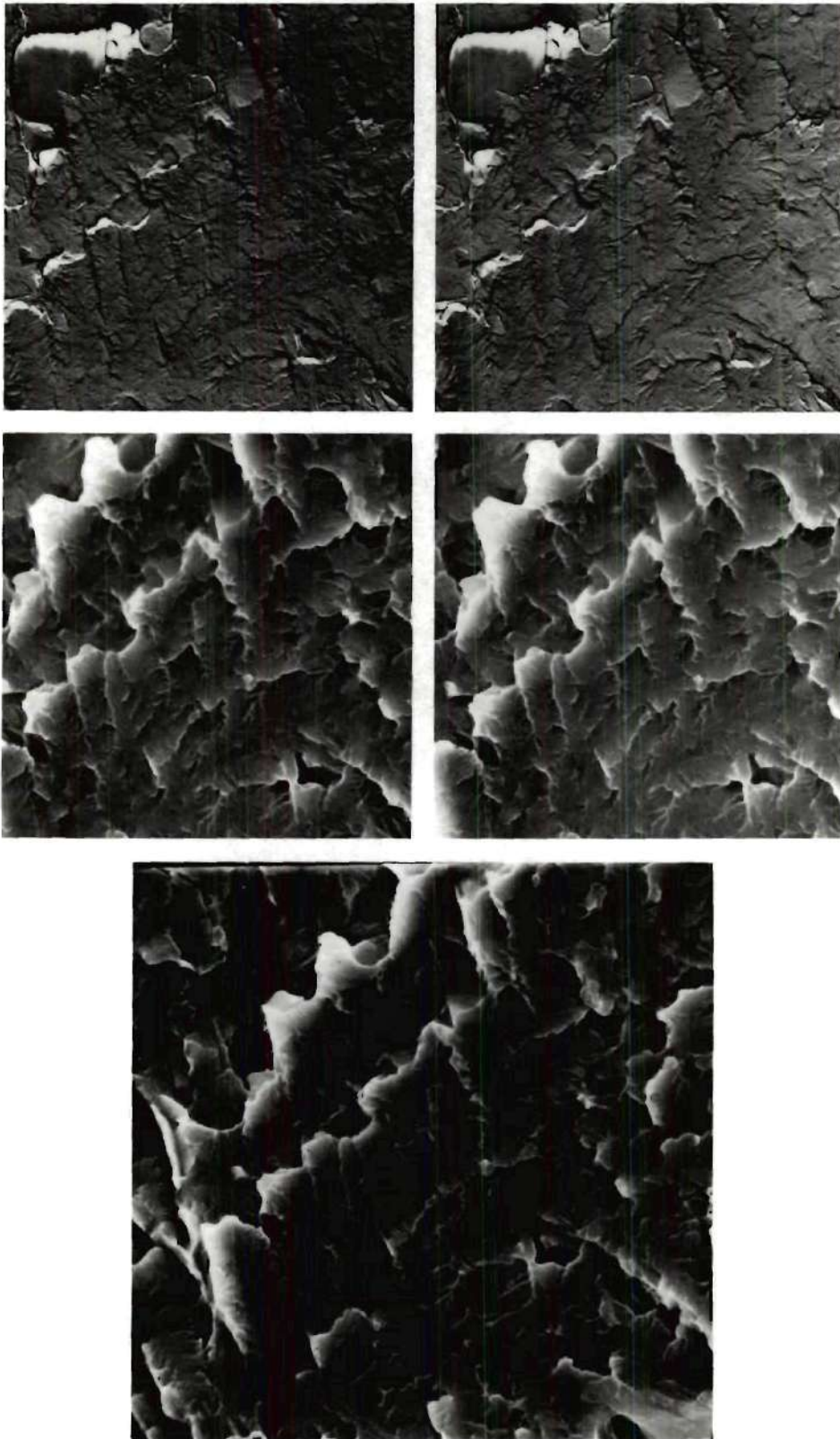


Figure 44. Comparison of TEM and SEM Fractography in Stress Corrosion of Ti 8-1-1 Alloy (on following page)

Material: Titanium; 8Al, 1Mo, 1V

Heat Treatment: Annealed

Type of Test: Stress corrosion

Ultimate Strength: 145,000 psi typical

Test Environment: 3½% NaCl in water at ambient temperature

Magnification of Fractographs: 4000X

Tilt of Single Scanning Micrograph: 30°

Appearance of Fracture: The fracture surface shows non-classic cleavage typical of stress corrosion cracking in this alloy.

Comparison Analysis: The transmission micrograph shows surface nicely.

There does not seem to be a good match between the replica and the surface. The scanning micrograph reveals a much rougher surface than indicated by the replica. It is evident that the replica has been flattened and that the features seen from the left to center are features of the steep wall leading up to the right hand feature as seen in the scanning micrograph.

The single tilted scanning micrograph shows the topography fairly well without the use of stereo.

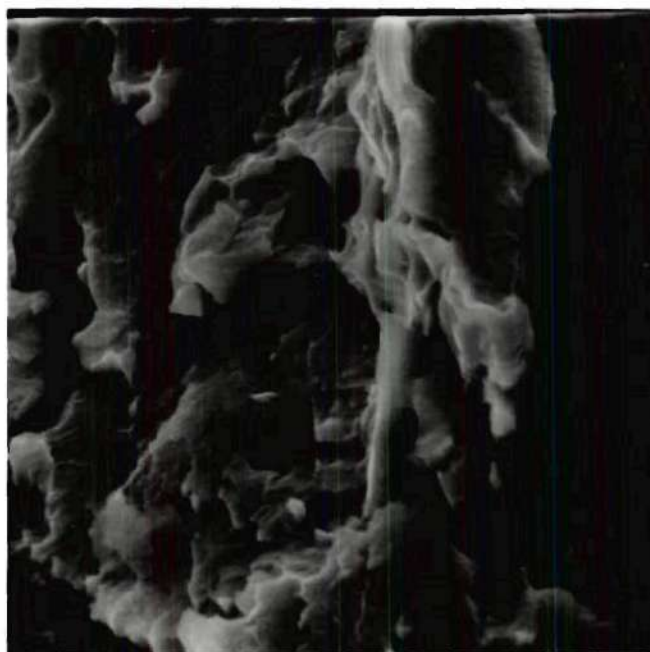
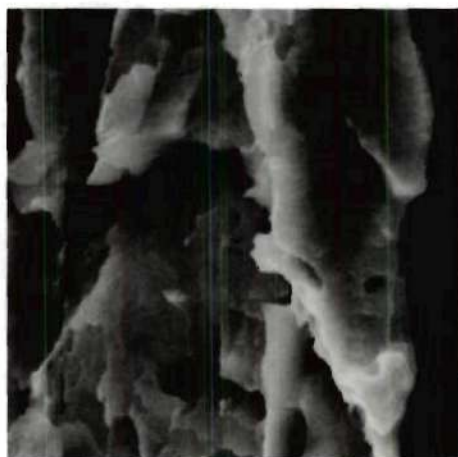
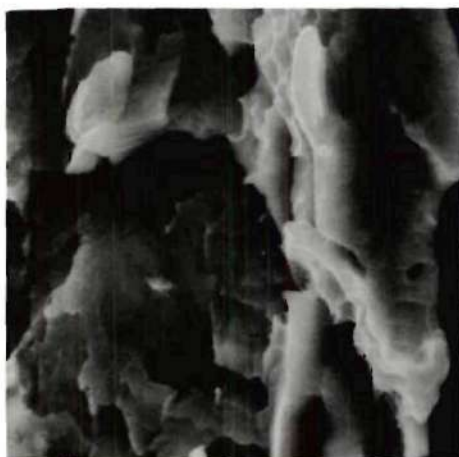


Figure 45. Comparison of TEM and SEM Fractography in Stress Corrosion of Ti 8-1-1 Alloy (on following page)

Material: Titanium; 8Al, 1Mo, 1V

Heat Treatment: Annealed

Type of Test: Stress corrosion

Ultimate Strength: 145,000 psi typical

Test Environment: 3½% NaCl in water at ambient temperature

Magnification of Fractographs: 4000X

Tilt of Single Scanning Micrograph: 30°

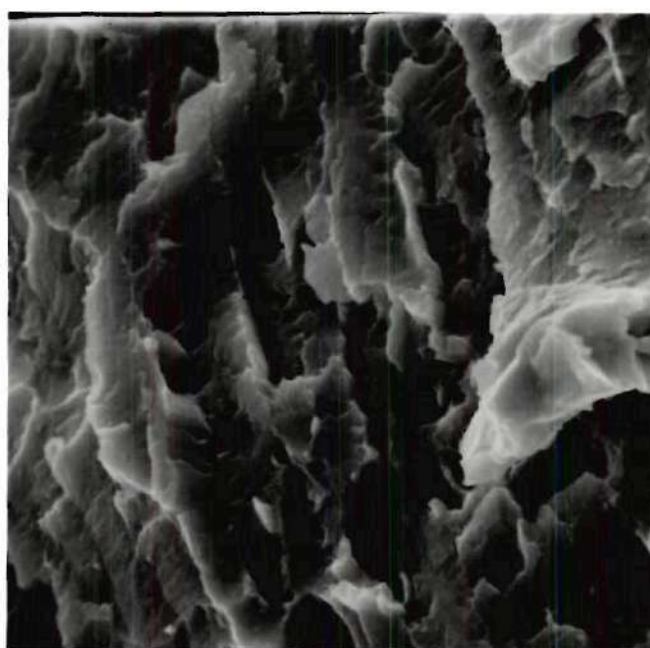
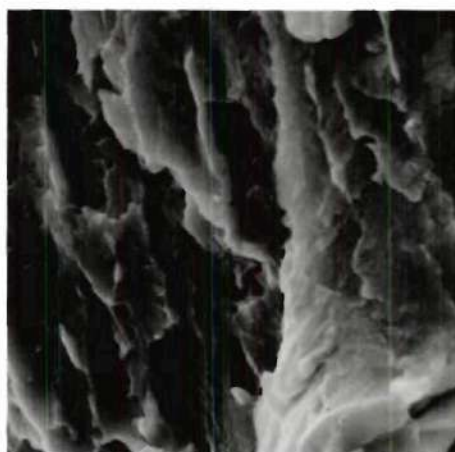
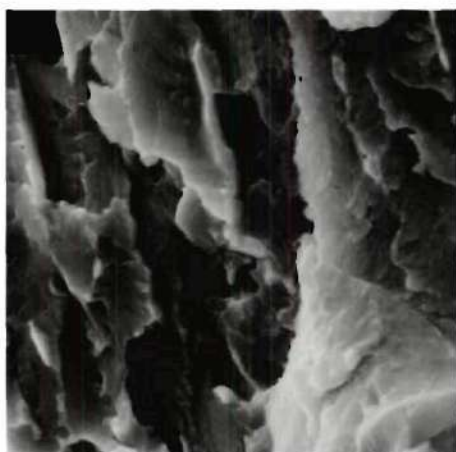
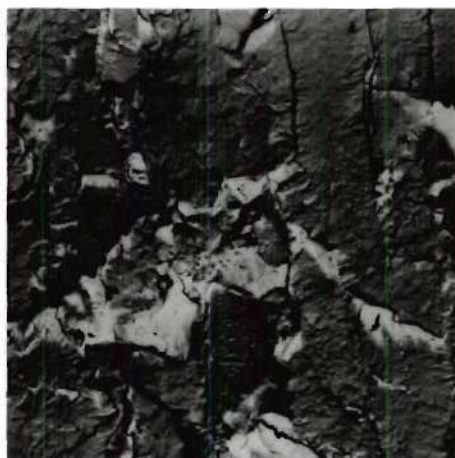
Appearance of Fracture: The fracture surface shows non-classic

cleavage typical of stress corrosion cracking in this alloy.

Comparison Analysis: The transmission micrograph shows the cleavage

surfaces. This area appears quite flat. The match is not too good between the replica and the surface. The scanning micrograph shows this area to be much rougher than indicated by the replica. It is evident the replica has flattened and some of the details seen in the replica are from the side of the steep wall which crosses the center of the scanning micrograph.

The single tilted scanning micrograph shows the topography moderately well without the use of stereo.



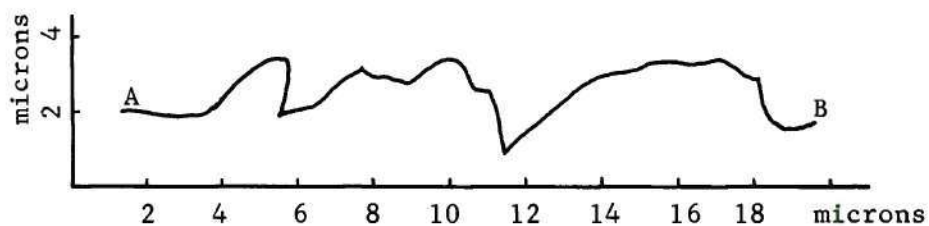
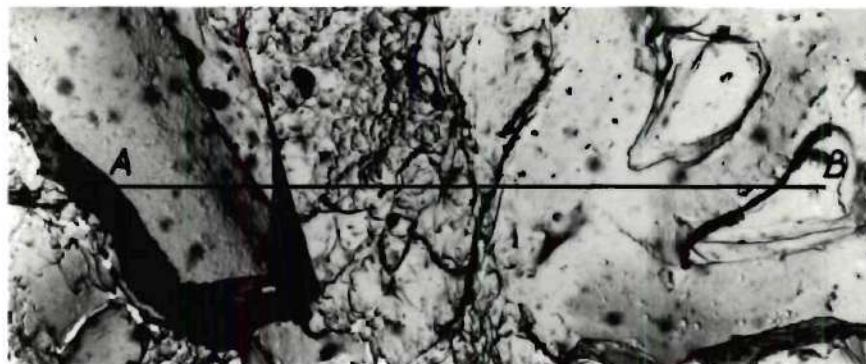
CHAPTER V

RESULTS AND CONCLUSION

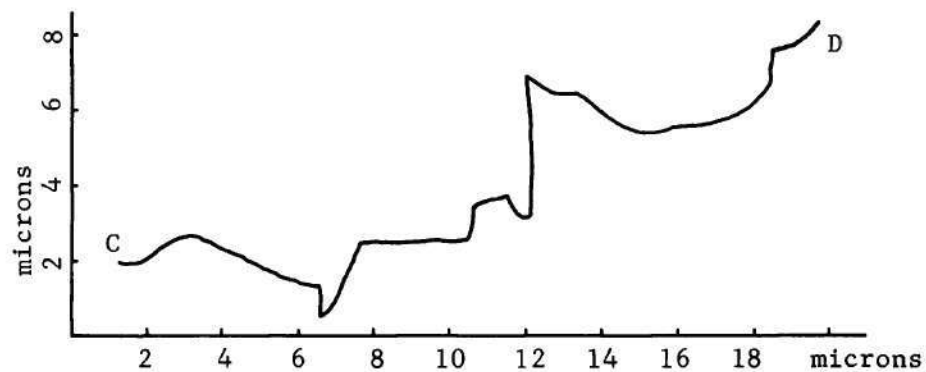
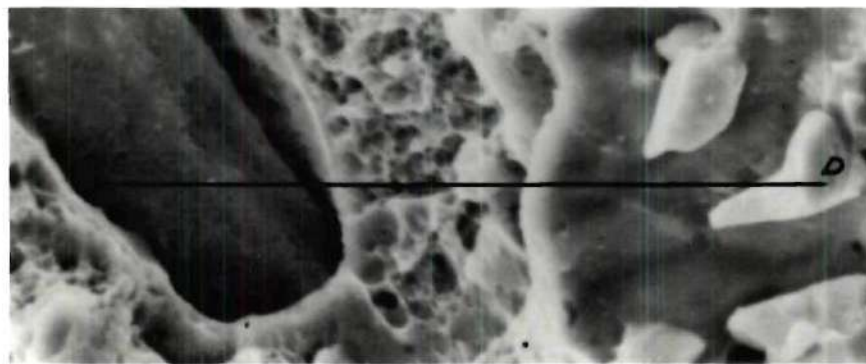
Comparisons reveal great differences in the apparent topography and resolution of the two methods used. The topography can be seen in all stereo pictures and topographic profiles are shown of Figure 7 in Figure 46. These profiles demonstrate clearly the collapse of the wall surrounding the upper center feature in the replica.

Many such artifacts as this collapse are seen in the comparisons made in this work and some, as in Figure 7, cannot be distinguished as such without the comparison with the scanning micrographs. The areas studied in this work were chosen at random so that the frequency with which these artifacts are seen in replicas of particular fracture types should represent the true frequency of occurrence of these artifacts in other replicas of respective fracture types.

The comparisons show that in replicas of fracture surfaces most steeply slopping areas collapse or fall over and are presented artifactually as much flatter. An example of this can be seen in Figure 34. Deep holes and cracks in the surfaces are difficult to replicate as seen in Figures 26 and 29. Many other features seen on the negative replicas are very difficult to properly interpret. On the other hand, the high resolution of the transmission micrographs shows fine surface detail which is not visible in the scanning micrographs. This is shown in Figure 27.



(a) Transmission Electron Micrograph and Topographic Drawing from Height Measurements Along Line AB.



(b) Scanning Electron Micrograph and Topographic Drawing from Height Measurements Along Line CD.

Figure 46. Topographic Comparison of Replica and Surface

The scanning micrographs show the true topography of the sample very well although as mentioned above some fine surface details which might be important to analysis are not resolved.

For the practical fractographer the scanning electron microscope provides the fastest method of fracture analysis, provided the sample may be cut to a suitable size. If the mode of fracture is immediately evident then his job is done. If, however, there is some question, he may have to resort to replication and transmission electron microscopy to see if the fine surface detail is meaningful. Many workers have had difficulty in distinguishing fatigue striations in the scanning electron microscope. They can however be resolved very well in certain cases as shown by the micrographs in this atlas. Generally enough detail is seen in the scanning electron microscope to identify the mode of fracture.

For the theoretical fractographer both transmission and scanning electron microscopy are necessary. The fine surface detail must be resolved but the true surface topography and the comparison to point out unrecognized replica artifacts are very important also. A general idea of surface topography can often be obtained from a single tilted scanning micrograph but stereo never leaves a doubt.

LITERATURE CITED

1. Réaumur, L'art de convertir le fer en acier, Paris, (1722).
2. A. Martens, Zeitschrift des Vereins deutscher Ingenieurure, 21, 11, (1878).
3. F. Osmond, C. Frémont, and G. Cartaud, Revue de Metallurgie, 1, 10, (1904).
4. A. Portevin, Rapports du Premier Congrès International de la Sécurité Aérienne, 1, 3, (1930).
5. A. Portevin, Metal Progress, 87, (June, 1931).
6. C. A. Zapffe and C. E. Sims, Metals Technology, 8, TP 1307, (1941).
7. C. A. Zapffe and G. A. Moore, Metals Technology, 10, TP 1553, (1943).
8. C. A. Zapffe and M. Clogg, Transactions, American Society for Metals, 34, 71 and 108, (1945).
9. C. A. Zapffe, Metal Progress, 50, 283, (1946).
10. C. A. Zapffe, Metal Progress, 51, 428, (1947).
11. C. A. Zapffe, Rev. Mét., 44, 9, (1947).
12. C. A. Zapffe, Trans. ASM, 41, 396, (1949).
13. C. A. Zapffe and C. D. Worden, Trans. ASM, 53, 958, (1951).
14. C. A. Zapffe and F. K. Landgraf, Rev. Mét., 48, 811, (1951).
15. A. Phillips, V. Kerlins, and B. V. Whiteson, Electron Fractography Handbook, Technical Report ML-TDR, 64-416, Wright Patterson Air Force Base, (1965).
16. G. Henry and J. Plateau, La Microfractographie, 3, Métaux (ed.).

OTHER REFERENCES

1. American Society for Testing and Materials, Electron Fractography, STP 436, (1968).
2. Burghard, Jr., H. C., Electron Fractography of Metals and Alloys, ASM-TR-H2.1-64.
3. Heidenreich, R. D., Fundamentals of Transmission Electron Microscopy, Interscience, New York, (1964).
4. Russ, J. C., "Comparison of Fractographic Techniques, Part I," Microstructures, 2, 1, (Dec.-Jan., 1971).
5. Russ, J. C., "Comparison of Fractographic Techniques, Part II," Microstructures, 2, 2, (Feb.-Mar., 1971).
6. Thornton, P. R., Scanning Electron Microscopy, Chapman and Hall, London, (1968).